Nidovirus RNA polymerases: Complex enzymes handling exceptional RNA genomes

Posthuma, C.C.; Velthuis, A.J.W. te; Snijder, E.J.

Virus Research 234 (2017) 58–73

Contents lists available at ScienceDirect

Virus Research

journal homepage: www.elsevier.com/locate/virusres

Review

Nidovirus RNA polymerases: Complex enzymes handling exceptional RNA genomes

Clara C. Posthuma[a,*,1], Aartjan J.W. te Velthuis[b,c,1], Eric J. Snijder[a,1]

[a] Molecular Virology Laboratory, Department of Medical Microbiology, Leiden University Medical Center, Leiden, the Netherlands
[b] Sir William Dunn School of Pathology, University of Oxford, South Parks Road, Oxford OX1 3RE, United Kingdom
[c] Clarendon Laboratory, Department of Physics, University of Oxford, Parks Road, Oxford OX1 3PU, United Kingdom

ARTICLE INFO

Article history:
Received 9 December 2016
Received in revised form 24 January 2017
Accepted 26 January 2017
Available online 6 February 2017

Keywords:
Coronavirus
Arterivirus
Replication and transcription complex
Polymerase fidelity
Processivity factors
Subgenomic mRNA synthesis

ABSTRACT

Coronaviruses and arteriviruses are distantly related human and animal pathogens that belong to the order *Nidovirales*. Nidoviruses are characterized by their polycistronic plus-stranded RNA genome, the production of subgenomic mRNAs and the conservation of a specific array of replicase domains, including key RNA-synthesizing enzymes. Coronaviruses (26–34 kilobases) have the largest known RNA genomes and their replication presumably requires a processive RNA-dependent RNA polymerase (RdRp) and enzymatic functions that suppress the consequences of the typically high error rate of viral RdRps. The arteriviruses have significantly smaller genomes and form an intriguing package with the coronaviruses to analyse viral RdRp evolution and function. The RdRp domain of nidoviruses resides in a cleavage product of the replicase polyprotein named non-structural protein (nsp) 12 in coronaviruses and nsp9 in arteriviruses. In all nidoviruses, the C-terminal RdRp domain is linked to a conserved N-terminal domain, which has been coined NiRAN (nidovirus RdRp-associated nucleotidyl transferase). Although no structural information is available, the functional characterization of the nidovirus RdRp and the larger enzyme complex of which it is part, has progressed significantly over the past decade. In coronaviruses several smaller, non-enzymatic nsps were characterized that direct RdRp function, while a 3′-to-5′ exoribonuclease activity in nsp14 was implicated in fidelity. In arteriviruses, the nsp1 subunit was found to maintain the balance between genome replication and subgenomic mRNA production. Understanding RdRp behaviour and interactions during RNA synthesis and subsequent processing will be key to rationalising the evolutionary success of nidoviruses and the development of antiviral strategies.

Contents

Abbreviations: 5-AZC, 5-azacytidine; 5-FU, 5-fluorouracil; AV, arterivirus; CBV3, coxsackievirus B3; CoV, coronavirus; EAV, equine arteritis virus; EM, electron microscopy; ExoN, exoribonuclease; FCoV, feline coronavirus; FMDV, foot and mouth disease virus; HCoV-229E, human coronavirus 229E; IMPDH, inosine-5′-monophosphate dehydrogenase; IVRA, *in vitro* RNA synthesis assay; kb, kilobases; M2H, mammalian 2-hybrid; MERS, Middle East respiratory syndrome; MHV, murine hepatitis coronavirus; NiRAN, nidovirus RdRp-associated nucleotidyltransferase; nsp, non-structural protein; ORF, open reading frame; PABP, Poly(A)-binding protein; PEDV, porcine epidemic diarrhea virus; PNS, post-nuclear supernatant; pp, polyprotein; PRRSV, porcine reproductive and respiratory syndrome virus; RBV, ribavirin; RdRp, RNA dependent RNA polymerase; RTC, replication and transcription complex; SARS, severe acute resporiatory syndrome; sg, subgenomic; ss, single-stranded; TGEV, transmissible gastroenteritis virus; TRS, transcription-regulatory sequence; ub, ubiquitin; wt, wild-type; Y2H, yeast 2-hybrid; ZBD, zinc-binding domain.

* Corresponding author.
E-mail address: c.c.posthuma@lumc.nl (C.C. Posthuma).
[1] These authors contributed equally.

http://dx.doi.org/10.1016/j.virusres.2017.01.023

1. Introduction

Positive-stranded RNA (+RNA) viruses that belong to the order *Nidovirales* infect a wide range of vertebrates (families *Arteriviridae* and *Coronaviridae*) or invertebrates (*Mesoniviridae* and *Roniviridae*) (de Groot et al., 2012; Lauber et al., 2012) and can have a significant economic and societal impact. For example, infections with the arterivirus (AV) porcine reproductive and respiratory syndrome virus (PRRSV) have severely affected the swine industry for almost three decades now (Holtkamp et al., 2013; Perez et al., 2015; Pileri and Mateu, 2016), whereas zoonotic coronaviruses (CoVs) have caused episodes of severe acute respiratory syndrome (SARS) and Middle East respiratory syndrome (MERS) in humans (Graham et al., 2013; Perlman and Netland, 2009) and may do so again (Menachery et al., 2015). Animal CoVs continue to emerge and cause great economic losses, as exemplified by the recent outbreaks of porcine deltacoronavirus and the porcine epidemic diarrhea virus (PEDV) in China and the United States (Choudhury et al., 2016; Weng et al., 2016; Zhang, 2016). Genetically, the nidoviruses constitute a monophyletic group that is characterized by common ancestry of their key replicative enzymes and associated similarities in genome organization and expression (Fig. 1A) (de Groot et al., 2012; Lauber et al., 2013). However, nidovirus genome sizes vary significantly, with AV genomes ranging from 13 to 16 kilobases (kb), mesonivirus genomes from 20 to 21 kb, and CoV genomes from 26 to 34 kb (Lauber et al., 2013). It has been postulated that this size variation reflects a long history of gradual genome expansion, during which the different nidovirus lineages adapted to their specific niches by acquiring a range of novel functions, encoded by domains that were either incorporated as additional genes or integrated into the large nidovirus replicase gene (Lauber et al., 2013).

In all nidoviruses, at least two-thirds of the capacity of the polycistronic genome is occupied by the two large open reading frames (ORFs; 1a and 1b) that together constitute the replicase gene (Fig. 1A). Both ORFs are translated directly from the viral genome and briefly overlap where a −1 ribosomal frameshift directs the expression of ORF1b to facilitate the formation of an ORF1ab-encoded polyprotein (pp1ab). Cleavage of the pp1a and pp1ab polyproteins by multiple intrinsic protease activities, in combination with −1 and −2 frameshifting in the nsp2 coding region in most arteriviruses with the exception of equine arteritis virus (EAV), results in the production of 13 to 17 non-structural proteins (nsps) (Fang et al., 2012; Li et al., 2014b; Snijder et al., 2013; Ziebuhr et al., 2000). The common ancestry of the extremely diverged nidovirus lineages is primarily reflected in the conservation of an array of 'core replicase domains' (Gorbalenya et al., 2006; Lauber et al., 2013; Snijder et al., 2016), which is composed of two *trans*-membrane proteins, the viral main protease, and – encoded downstream of the ORF1a/1b frameshift site – the RNA-dependent RNA polymerase (RdRp)- and helicase-containing subunits (Fig. 1B), with the canonical RdRp domain residing in CoV nsp12 and AV nsp9. Nidovirus genomes are thought to have expanded gradually by gene duplication and the acquisition of novel domains (Lauber et al., 2013). During this process, specific innovations may have enabled them to explore an unprecedented evolutionary space and adapt to a wide variety of host organisms, including mammals, birds, fish, insects and crustaceans. In particular, the general genome size restrictions of RNA viruses, commonly attributed to the poor nucleotide incorporation fidelity of the viral RdRp domain, may have been mitigated by the acquisition of compensatory enzymatic functions (Deng et al., 2014; Eckerle et al., 2010; Eckerle et al., 2007; Gorbalenya et al., 2006; Snijder et al., 2003). Consequently, some nidovirus nsps contain a unique set of activities not seen in other +RNA viruses (discussed *e.g.* in Sections 8 and 11 in more detail). Imaging and biochemical characterization of nidovirus nsps have shown that they are targeted to specific virus-induced membrane structures (reviewed in (Hagemeijer et al., 2012; Neuman et al., 2014; van der Hoeven et al., 2016)) where they assemble into a so-called replication and transcription complex (RTC; see (Neuman et al., 2014; Snijder et al., 2016; Subissi et al., 2014a) for reviews).

The RNA-templated synthesis of new RNA by the viral RNA polymerase is arguably the key step in the infection cycle of all RNA viruses. In the case of nidoviruses and their polycistronic genomes, RNA synthesis entails not only genome amplification but also the synthesis of a nested set of subgenomic (sg) mRNAs (Fig. 1A; reviewed in (Pasternak et al., 2006; Sawicki et al., 2007; Sola et al., 2011). The sg mRNAs serve to make the genes downstream of the nidovirus replicase ORFs 1a and 1b accessible for translation. These ORFs encode structural and so-called 'accessory' proteins, which are often dispensable for replication *in vitro*, but important for *e.g.* immune evasion and pathogenesis *in vivo* (Liu et al., 2014; Weiss and Leibowitz, 2011). For the purpose of this review, we will refer to the process of sg mRNA synthesis as 'transcription'; the underlying mechanisms will be discussed in more detail in Section 10.

Each nidoviral sg mRNA is produced from a complementary subgenome-length template. Minus strand RNA synthesis can be either continuous (producing a full-length minus-strand template for genome replication) or discontinuous to produce the subgenome-length templates for the production of the sg mRNAs (Sawicki and Sawicki, 1995; Sethna et al., 1989). In addition to the overall RNA structure of the genome and transcription-specific protein factors, conserved transcription-regulatory sequences (TRSs) in the genomic template are thought to be the prime trigger and guiding elements that make the nidovirus RTC synthesize a subgenome-length rather than a full-length minus strand. Thus, the TRSs constitute one class of *cis*-acting RNA signals with which the nidovirus RTC needs to interact, although we note that this feature has mainly been addressed from the RNA side (*e.g.*, by site-directed mutagenesis of TRSs) (Dufour et al., 2011; Pasternak et al., 2001; Zheng et al., 2014; Zuniga et al., 2004). The same essentially applies to the major *cis*-acting RNA elements that constitute the initiation sites for minus and plus strand RNA synthesis near the 3′ end of the plus and minus strand, respectively. Indeed, in both CoV and AV genomes, a number of primary and higher-order structural features have been identified and studied, including sev-

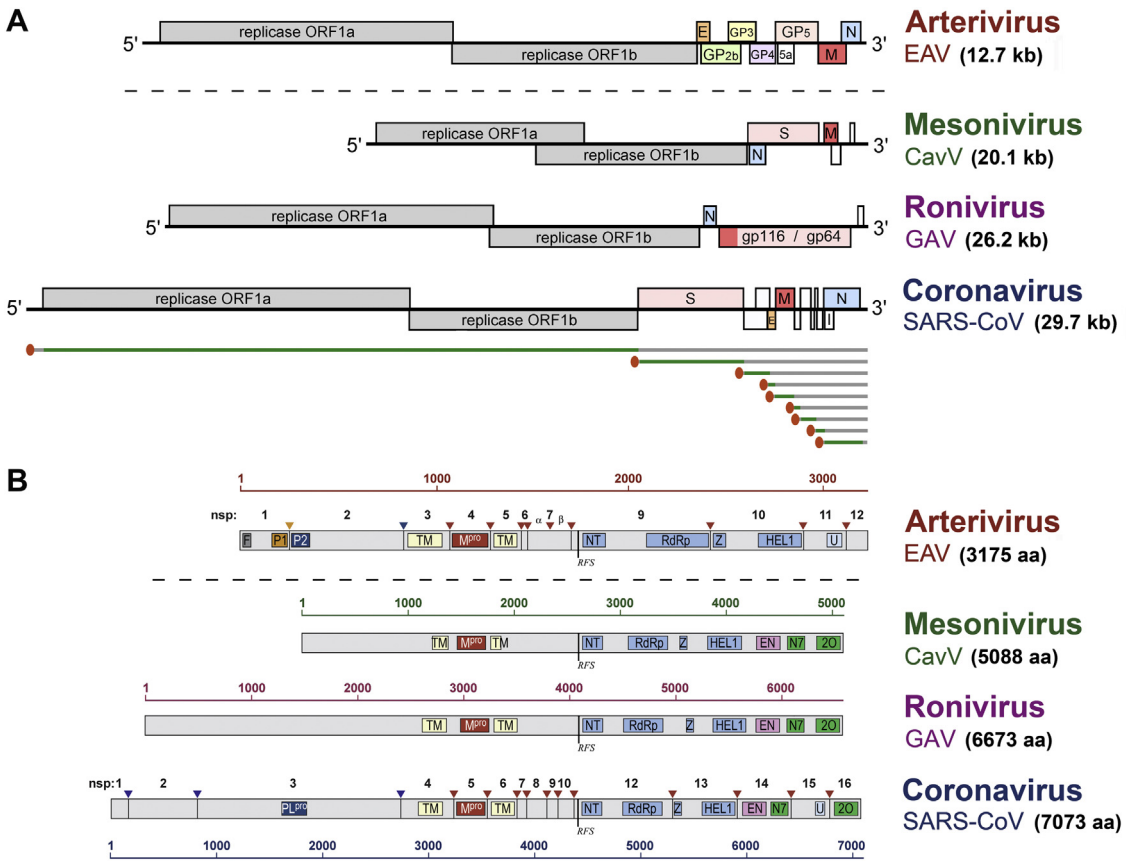

Fig. 1. Nidovirus genome organization and the core replicase domains. (A) Genome organization of representatives of the four major nidovirus lineages (CavV, Cavally virus; GAV, gill-associated virus; note that the EAV genome is drawn to a different scale). For each genome, the known open reading frames (ORFs) are indicated with the replicase ORFs 1a and 1b depicted in grey and structural protein genes depicted in different colours. ORFs encoding 'accessory proteins' (in SARS-CoV) or poorly characterized products are depicted in white. To illustrate the principle of subgenomic mRNA synthesis, as employed by all nidoviruses, the nested set structure and composition of the mRNAs is summarized for SARS-CoV, with the common 5′ leader sequence indicated in red and the translated part of the genome and each of the subgenomic mRNAs depicted in green. See main text for more details. (B) Domain organization of the pp1ab replicase polyprotein for the four major nidovirus lineages (note that the AV protein is drawn to a different scale). Proteolytic cleavages and non-structural protein numbering are indicated for EAV and SARS-CoV. The scheme highlights the conservation of the so-called nidovirus 'core replicase', consisting of the ORF1a-encoded main protease (Mpro) flanked by two transmembrane (TM) domains, followed by the ORF1b-encoded NiRAN nucleotidyl transferase (NT), RNA polymerase (RdRp), zinc binding domain (Z) and superfamily 1 helicase (HEL1). Accessory (papain-like) protease domains and their cleavage sites are indicated for EAV and SARS-CoV (P1, P2, PLpro). The zinc-finger domain (F) in EAV nsp1 that is crucial for subgenomic mRNA synthesis (see text) is also highlighted. The C-terminal part of pp1ab encodes a number of enzymatic domains that are not strictly conserved among all nidovirus lineages: U, endoribonuclease, conserved in vertebrate nidoviruses; EN, exoribonuclease (ExoN) conserved in nidoviruses with genome sizes >20 kb (see text); N7- and 2′-O methyl transferases (N7 and 2O) involved in cap modification (not identified in AVs).

eral RNA hairpins and pseudoknots. The importance of multiple of these elements is supported by bioinformatics (conservation), biochemical probing, and site-directed mutagenesis. For an overview of the structure and function of the RNA elements that have been implicated in CoV or AV replication and transcription, the reader is referred to detailed reviews that have been published elsewhere (Madhugiri et al., 2016; Masters, 2007; Snijder et al., 2013; Sola et al., 2011; Yang and Leibowitz, 2015). However, it has remained largely unclear whether these elements interact with the RdRp domain-containing subunit directly or with other components of the RTC, as for example reported by Züst et al. who observed that second-site mutations in the small nsp8 and nsp9 subunits of the RTC could compensate for mutations in conserved RNA sequences near the genomic 3′ end of the murine hepatitis coronavirus (MHV) genome (Züst et al., 2008). In the case of the 5′-proximal domain of the genomic RNA (or its minus-stranded counterpart), functional studies have been complicated by the fact that RNA signals for replication, transcription, translation and (potentially) packaging may be overlapping and difficult to separate, both physically and functionally.

In this review, we will focus mainly on 'the protein side' of nidovirus RNA synthesis, and what is known about the initiation of RNA synthesis by nidovirus RNA polymerases. The ability of the nidovirus RTC to direct the various processes of RNA synthesis outlined above critically relies on the activity of a canonical RdRp domain, which resides in nsp12 in CoVs and in nsp9 in AVs. These replicase subunits, which also carry a unique and nidovirus-specific N-terminal extension, are believed to catalyse the nucleotide condensation reaction that drives replication and transcription. Given their pivotal role in viral replication and the efficacy of using polymerase inhibitors to combat other virus infections, AV nsp9 and CoV nsp12 are also considered an important target for rational drug design. Unfortunately, these nsps have remained refractory to structural analyses so far, but significant advances in our understanding of these enzymes and their co-factors have been made using bioinformatics, biochemical and molecular virological approaches, in particular for AVs and CoVs, as we will summarize below.

2. General features of nidovirus RNA polymerase subunits: two domains with distinct activities

In all nidoviruses, the RdRp-containing subunit consists of at least two domains (Fig. 2A): a nidovirus-specific N-terminal

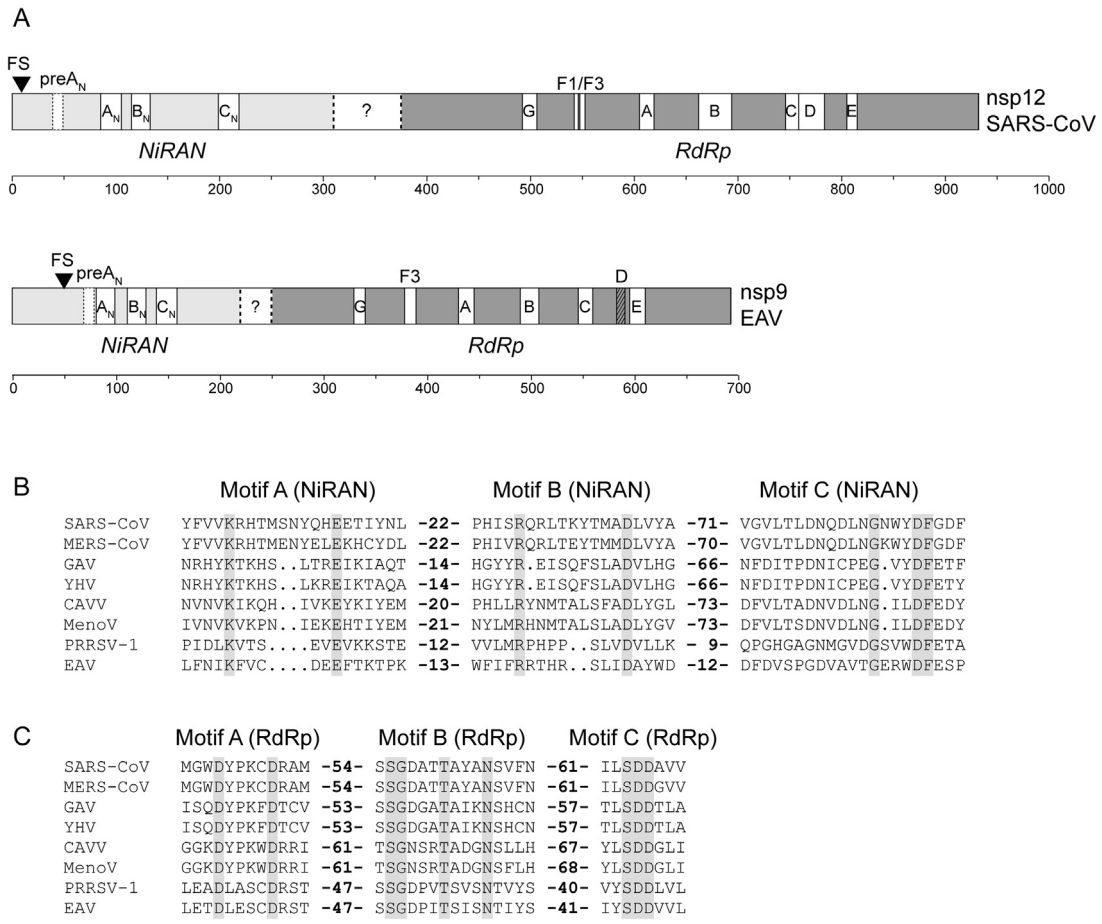

B

	Motif A (NiRAN)		Motif B (NiRAN)		Motif C (NiRAN)
SARS-CoV	YFVVKRHTMSNYQHEETIYNL	-22-	PHISRQRLTKYTMADLVYA	-71-	VGVLTLDNQDLNGNWYDFGDF
MERS-CoV	YFVVKRHTMENYELEKHCYDL	-22-	PHIVRQRLTEYTMMDLVYA	-70-	VGVLTLDNQDLNGKWYDFGDF
GAV	NRHYKTKHS..LTREIKIAQT	-14-	HGYYR.EISQFSLADVLHG	-66-	NFDITPDNICPEG.VYDFETF
YHV	NRHYKTKHS..LKREIKTAQA	-14-	HGYYR.EISQFSLADVLHG	-66-	NFDITPDNICPEG.VYDFETY
CAVV	NVNVKIKQH..IVKEYKIYEM	-20-	PHLLRYNMTALSFADLYGL	-73-	DFVLTADNVDLNG.ILDFEDY
MenoV	IVNVKVKPN..IEKEHTIYEM	-21-	NYLMRHNMTALSLADLYGV	-73-	DFVLTSDNVDLNG.ILDFEDY
PRRSV-1	PIDLKVTS....EVEVKKSTE	-12-	VVLMRPHPP..SLVDVLLK	- 9-	QPGHGAGNMGVDGSVWDFETA
EAV	LFNIKFVC....DEEFTKTPK	-13-	WFIFRRTHR..SLIDAYWD	-12-	DFDVSPGDVAVTGERWDFESP

C

	Motif A (RdRp)		Motif B (RdRp)		Motif C (RdRp)
SARS-CoV	MGWDYPKCDRAM	-54-	SSGDATTAYANSVFN	-61-	ILSDDAVV
MERS-CoV	MGWDYPKCDRAM	-54-	SSGDATTAYANSVFN	-61-	ILSDDGVV
GAV	ISQDYPKFDTCV	-53-	SSGDGATAIKNSHCN	-57-	TLSDDTLA
YHV	ISQDYPKFDTCV	-53-	SSGDGATAIKNSHCN	-57-	TLSDDTLA
CAVV	GGKDYPKWDRRI	-61-	TSGNSRTADGNSLLH	-67-	YLSDDGLI
MenoV	GGKDYPKWDRRI	-61-	TSGNSRTADGNSFLH	-68-	YLSDDGLI
PRRSV-1	LEADLASCDRST	-47-	SSGDPVTSVSNTVYS	-40-	VYSDDLVL
EAV	LETDLESCDRST	-47-	SSGDPITSISNTIYS	-41-	IYSDDVVL

Fig. 2. Schematic representation of nsp12 from SARS-CoV and nsp9 from EAV. A) The position of NiRAN (light grey), the RdRp domain (dark grey) and the respective motifs (white boxes; subscript "N" was added to NiRAN motifs to dicriminate them from RdRp motifs) are indicated in the figure. The exact C-terminal border of NiRAN, as well as the N-terminal border of the RdRp are not defined yet and are indicated with dashed lines. The position of ribosomal frameshifting is indicated with a triangle; translation of the preceding ORF1a products terminates shortly downstream the frameshift site (SARS-CoV nsp11 within 4 amino acids, EAV nsp8 within 1 amino acid, not indicated in the figure). NiRAN and RdRp motifs are displayed as white boxes in the figure, based on (Lehmann et al., 2015a) for NiRAN motifs, and (Xu et al., 2003) (SARS-CoV) or (Beerens et al., 2007) (EAV) for the RdRp motifs. Note that Motif D was not defined for EAV nsp9 in Beerens et al. and that the approximate position is indicated as a dashed box. The rulers indicate amino acid positions in the proteins. Question mark indicates part of the nsp that may represent a linking domain or a domain with an additional (unknown) function. B) Alignment of NiRAN motifs A, B and C from eight representative nidoviruses from all 4 families (Modified from (Lehmann et al., 2015a)). C) Alignment of RdRp motifs A, B and C from the same nidoviruses. Completely conserved residues are indicated in grey boxes. SARS-CoV, SARS coronavirus Frankfurt 1 (AY291315; *Coronaviridae*); MERS-CoV, Middle East respiratory syndrome coronavirus EMC/2012 (JX869059.2; *Coronaviridae*); GAV, Gill-associated virus (AF227196; *Roniviridae*); YHV, yellow head virus (EU487200; *Roniviridae*); CAVV, Cavally virus (HM746600; *Mesoniviridae*); MenoV, Meno virus (JQ957873; *Mesoniviridae*); PRRSV-1, porcine reproductive and respiratory syndrome virus, European genotype (GU737264.2; *Arteriviridae*). EAV, Equine arteritis virus (DQ846750; *Arteriviridae*).

domain is followed by a canonical RdRp domain occupying the C-terminal two-thirds of the protein (Gorbalenya et al., 1989; Xu et al., 2003). Although the presence of this N-terminal extension was first recognized when the replicase polyprotein cleavage sites were predicted over 25 years ago (Gorbalenya et al., 1989), an enzymatic activity (nucleotidylation) was assigned to it only recently. The domain is now referred to as the nidovirus RdRp-associated nucleotidyltransferase (NiRAN) domain (Lehmann et al., 2015a) (Fig. 2B), and it will be discussed in more detail in Section 8. As the C-terminal border of NiRAN is difficult to define, yet another domain (approximately 50–175 amino acids for AV and CoV, respectively; Fig. 2A) may turn out to connect the NiRAN and RdRp domains (Lehmann et al., 2015a).

RdRp domains include six canonical conserved motifs, named A to F (Figs. 2C and 3A), that are involved in template and substrate recognition and the catalysis of nucleotide condensation (Poch et al., 1989; te Velthuis, 2014). Nucleotide condensation particularly depends on motifs A and C, which assist in coordinating the two metal ions in the active site (Alphonse and Ghose, 2017; te Velthuis, 2014). Nidovirus RdRp domains were first identified by sequence comparison with known RdRp domains from other virus groups, revealing an SDD sequence (instead of the usual GDD signature found in other positive-strand RNA virus RdRp domains) as the key residues of motif C (den Boon et al., 1991; Gorbalenya et al., 1989; Snijder et al., 1990) (residues 759-761 in SARS-CoV) and D618 and D623 as the conserved aspartate residues of motif A of SARS-CoV nsp12. These residues correspond with D445 and D450 in motif A and SDD at positions 559-561 in nsp9 of the AV prototype EAV. Two decades later, the mutational analysis of conserved RdRp domain residues confirmed that the catalytic aspartates of motifs A and C are important for RNA polymerase activity and viral RNA synthesis (Ahn et al., 2012; Lehmann et al., 2016; Subissi et al., 2014b; te Velthuis et al., 2010a). In addition to the essential RdRp domain motifs mentioned above, CoV nsp12 has a motif G, which is considered a signature sequence for primer-dependent RNA polymerases (Gorbalenya et al., 2002; Xu et al., 2003). Remarkably, this motif is only partially conserved in the AV nsp9 (Beerens et al., 2007).

A structural prediction for the SARS-CoV RdRp domain was published as early as 2003 (Xu et al., 2003) (Fig. 3B), yet experimental studies to support this model have been greatly hampered by difficulties with attempts to stably express and purify CoV nsp12. As a result, the crystal structure of the CoV RNA polymerase remains

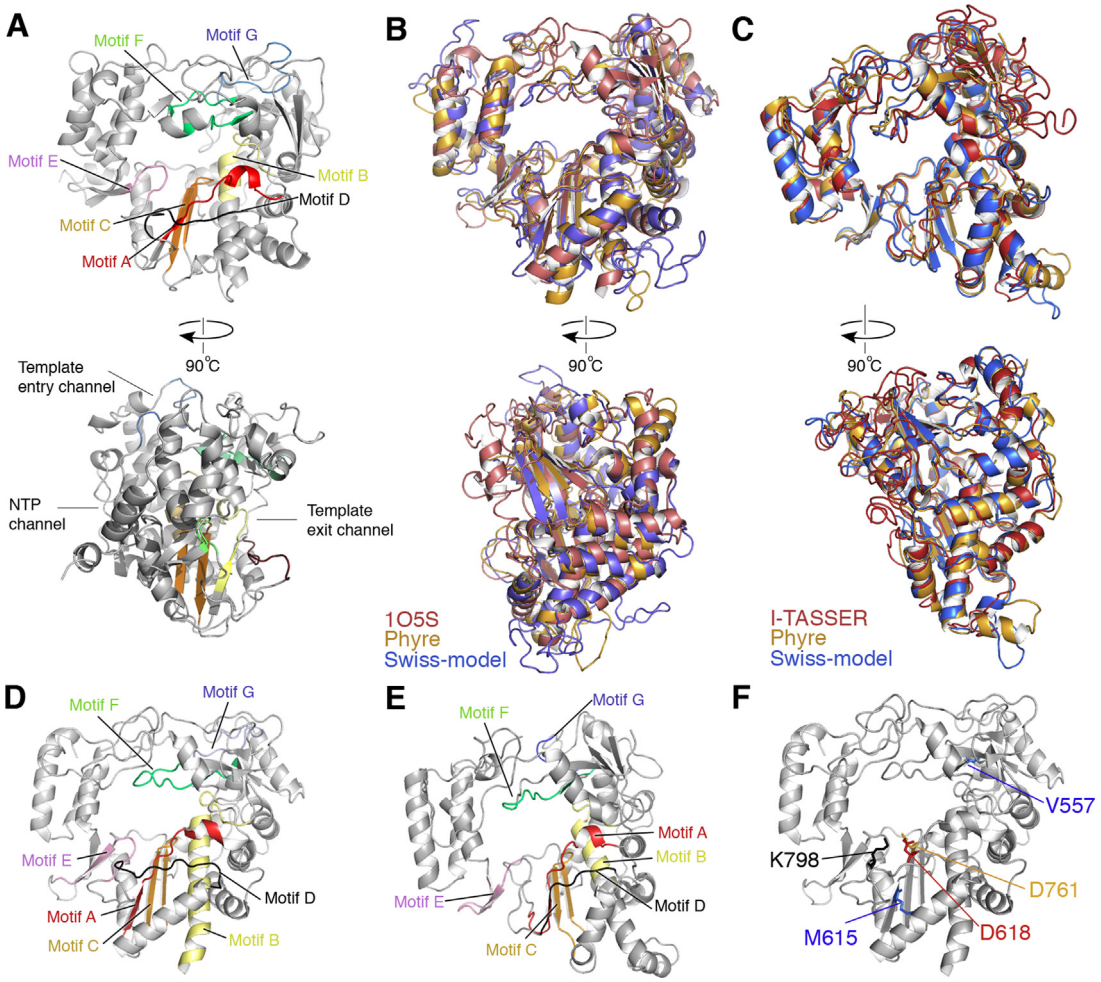

Fig. 3. Models of the nidovirus RdRps. A) Structure of the FMDV RdRp (pdb 2E9R). In the top panel, conserved polymerase motifs A-F are indicated. In the bottom panel, the template entry, template exit and NTP entry channels are indicated. B) Models of the SARS-CoV nsp12 RdRp generated by Swiss-Model and Phyre2 superposed on the model 1O5S (Xu et al., 2003). All three models are based on the C-terminal polymerase domain and excluded the N-terminal NiRAN domain. All models show an overall similar fold. Differences exist in the fingers subdomain and surface loops of the thumb subdomain. C) Superposed models of the EAV nsp9 RdRp generated by use of I-TASSER, Swiss-Model and Phyre2. Overall, all three models show a very similar fold, with small differences in the fingers subdomain. D) Motifs of the polymerase domain of SARS-CoV nsp12 indicated on the structural model 1O5S (Xu et al., 2003). E) Motifs of the polymerase domain of EAV nsp9 that was generated using Phyre2. F) Key active site and fidelity residues indicated on the model of polymerase domain of SARS-CoV nsp12 1O5S.

to be solved and its biochemical characterization in a very early stage. Unfortunately, the situation is not much different for the AV RNA polymerase. Most of our current understanding of the structural and enzymatic features of the nidovirus RNA polymerase/RTC is based exclusively on studies with SARS-CoV, which was targeted by a number of laboratories following the 2003 outbreak.

3. Structural models of nidovirus RdRps

To date, no cryo-EM or crystallographic structures of CoV nsp12 or AV nsp9 are available. However, using sequence alignments, secondary structure predictions and homology modelling, the molecular structure of the nsp12 subunit of SARS-CoV (Xu et al., 2003) (Fig. 3B) and MHV (Sexton et al., 2016) has been predicted. In case of the former, a model could be reliably generated for its conserved RdRp domain, based on a careful alignment of amino acids 388–890 to known polymerase sequences (Xu et al., 2003); Fig. 3B. Similar structures for SARS-CoV nsp12 are predicted by online tools like Swiss-Model (Biasini et al., 2014) and Phyre2 (Kelley et al., 2015) (Fig. 3B). However, no structural predictions are possible for the N-terminal domain of nsp12, which contains the NiRAN domain, and the C-terminal tail of the RdRp domain (amino acids 891–932 in SARS-CoV nsp12). Likewise, only the C-terminal RdRp domain of the AV nsp9 sequence can be modelled at present, as depicted in Fig. 3C for EAV.

An analysis of the predicted CoV RdRp domain architecture using three models (Fig. 3B) revealed a right-handed fold that consists of thumb, palm and fingers subdomains, similar to known crystal structures of RdRp domains or complete RNA polymerases (shown for foot and mouth disease virus (FMDV) in Fig. 3A). The models also predict the presence of a single-stranded (ss) RNA entry channel at the top of the polymerase and an NTP entry channel at the rear (Fig. 3). The duplex that is formed as the RNA polymerase catalyses nucleotide condensation, thus consisting of the nascent RNA product and the viral template, likely leaves the enzyme *via* a relatively wide exit channel at the front of the molecule. This predicted three-channel architecture would make the nidovirus RNA polymerase comparable to other +RNA-viral RNA polymerases, but different from the RNA polymerases of negative-stranded RNA viruses, which are believed to have separate exit channels for the template and nascent strand (Pflug et al., 2017; Reguera et al., 2016; te Velthuis and Fodor, 2016). Putative channels similar to those predicted for the CoV nsp12 RdRp domain can be seen in the models of the EAV nsp9 RdRp domain generated with the prediction tools Swiss-Model, Phyre2 and I-TASSER (Yang et al., 2015) (Fig. 3C), in line with earlier sequence analyses suggesting that

the overall molecular architecture is conserved among nidovirus RdRp domains (Beerens et al., 2007). In neither the CoV nor the AV RdRp domain model there is evidence for the presence of a priming-loop or similar initiation platform, which is typically required for *de novo* initiation on the 3′ terminus of the viral RNA (te Velthuis, 2014). This is in line with the presence of (a partial) motif G (see above) and together these features may have important functional implications for the initiation of viral RNA synthesis.

In both the CoV nsp12 and EAV nsp9 RdRp domain models, the three substrate channels converge at the beta sheets of the palm subdomain. Here the catalytic aspartates of motifs A and C coordinate the catalytic ions that are essential for the nucleotide condensation reaction (te Velthuis, 2014) (Fig. 3D and E). As described for other RdRp domains, the key lysine of motif D, which likely acts as general acid during catalysis (Castro et al., 2009), is located near the entrance of the NTP channel. Further functional predictions about the CoV RNA polymerase come from an alignment of a Phyre2-based molecular model of MHV nsp12 with the crystal structures of the RdRp domains of coxsackievirus B3 (CVB3) and poliovirus (Sexton et al., 2016). In particular, this study identified V553 and M611 (homologs of SARS-CoV nsp12 residues V557 and M615, Fig. 3F) as putative equivalents of the CVB3 RdRp residues I176 and I230, which are known to be involved in RdRp fidelity. Subsequent mutation of these residues to isoleucine (V553I) and phenylalanine (M611F) in the virus conferred resistance to 5-fluorouracil (5-FU) and 5-azacytidine (5-AZC), or 5-FU only, respectively (Sexton et al., 2016).

4. *In vitro* RdRp activity of the CoV nsp12

The first published attempts to purify a CoV nsp12 employed an N-terminal GST-fusion with SARS-CoV nsp12, which yielded a recombinant protein with poor solubility and stability (Cheng et al., 2005). Since then, advances have been made to improve the stability and yield of SARS-CoV nsp12 by using codon optimization, different purification tags at the N- or C-terminus, or the addition of an N-terminal, cleavable ubiquitin (ub) fusion partner (in combination with a C-terminal His_6-tag) (Ahn et al., 2012; Subissi et al., 2014b; te Velthuis et al., 2010a). Bacterial expression of the latter (*i.e.*, ub-nsp12-His_6) still resulted in an unstable protein, but co-expression of the ubiquitin protease Ubp1, which can hydrolyse the ub-nsp12 fusion site to produce a recombinant nsp12-His_6 containing the natural nsp12 N-terminus, significantly improved its stability (te Velthuis et al., 2010a). The C-terminal His_6-tag proved suitable to purify nsp12 from *E. coli* without a significant effect on the stability of the enzyme. Overall, these results suggested that, as for the poliovirus RNA polymerase $3D^{pol}$ (Thompson and Peersen, 2004), the N-terminus of nsp12 or, alternatively, the proper folding of the NiRAN domain which is not present in $3D^{pol}$, is important for the stability and possibly also the activity of nsp12 (te Velthuis et al., 2010a).

Analysis of the CoV nsp12 amino acid sequence using alignments and molecular modelling predicted that the enzyme lacks a priming loop or other initiation platform that would promote *de novo* initiation of RNA synthesis (see above). Since motif G, a presumed hallmark of primer-dependent polymerases (Gorbalenya et al., 2002; Xu et al., 2003), was identified in the nsp12 sequence and structural model (Figs. 2A and 3B), it was assumed that a primer would be required for the initiation of RNA synthesis by nsp12. Studies from both Cheng et al. and te Velthuis et al. showed that the activity of recombinant SARS-CoV GST-nsp12 or nsp12-His_6 was indeed primer-dependent in the presence of Mg^{2+} (Cheng et al., 2005; te Velthuis et al., 2010a). By contrast, Ahn et al. found that recombinant SARS-CoV nsp12 with an N-terminal His_6-tag (His_6-nsp12) required high concentrations of Mn^{2+}. Under these conditions, the enzyme was also able to initiate *de novo* on homopolymeric templates and a sequence representing the 3′ terminus of the viral genome (Ahn et al., 2012). Likewise, His_6-nsp12 was able to synthesize relatively long RNA products in the presence of Mn^{2+} (Ahn et al., 2012). The activity of nsp12-His_6 on templates longer than 20 nucleotides was not tested (te Velthuis et al., 2010a). Curiously, the most recent study on recombinant SARS-CoV nsp12 (containing a C-terminal strep-tag) did not find any primer extension, *de novo* initiation activity, or binding (using 1 μM of nsp12-strep) to a primed RNA template (Subissi et al., 2014b). By contrast, the nsp12-His_6 variant was found to bind RNA with an apparent Kd of ~0.1 μM (te Velthuis et al., 2010a).

The limited reproducibility of these biochemical observations and the scant support for substantial processivity of nsp12 are in stark contrast with the fact that the CoV RNA polymerase is required to replicate and transcribe a ~30-kb genome during infection. Technical differences between these studies (*e.g.* regarding the constructs and templates used) may have contributed to the mostly contradictory results. Nevertheless, together the observations teach us that the activity of nsp12 alone must be relatively weak and sensitive to the presence of purification tags, buffer conditions and the simplicity of the template. It is likely that CoV nsp12 requires additional factors that improve its RNA polymerase activity and there is indeed evidence that other nsps fulfil this role (see below) (Subissi et al., 2014b).

5. CoV nsp8: primase or not?

In a study aimed at finding putative interaction partners for nsp12, a second RNA polymerase activity was reported to be associated with SARS-CoV nsp8, a 22-kDa protein encoded in ORF1a (Imbert et al., 2006). This activity, which would be unique among RNA viruses, was observed to initiate RNA synthesis in a primer-independent manner on templates containing cytidine-rich sequences *in vitro* and to generate products of approximately 6 nt in length (Imbert et al., 2006). Together with the assumption based on comparative genomics that nsp12 is a primer-dependent RNA polymerase (see above), nsp8 was thus proposed to function as a primase, presumably generating the initiation substrate for nsp12.

In subsequent biochemical analyses, it was found that the N-terminus of SARS-CoV nsp8 modulates its oligomerization and polymerase activity (te Velthuis et al., 2012; Xiao et al., 2012). Moreover, proteolytic cleavage of an inactive nsp8 containing an N-terminal ubiquitin- and C-terminal His_6-tag showed that its nucleotide condensation abilities (*i.e. de novo* synthesis but also primer extension activity) can be activated by the removal of the terminal tags. These observations are in line with experiments showing that nsp8 appears to be largely inactive in the context of the precursor polyproteins nsp7-8 and nsp7-10 (te Velthuis et al., 2012; Xiao et al., 2012) and together they suggest that the (faithful) processing of nsp8 can affect and potentially regulate the activity of nsp8 in the complexes in which it resides in infected cells. We note, however, that the ability of nsp8 to extend primer-template duplexes with [α-^{32}P]ATP could not be confirmed in a subsequent study using a radiolabeled primer (Subissi et al., 2014b). The *de novo* RNA synthesis activity of nsp8 was not addressed in this study.

The structure of nsp8 alone is presently unknown, but it is likely that it forms oligomers based on gel shift, electron microscopy (EM) and gel filtration studies (te Velthuis et al., 2012; Zhai et al., 2005). The involvement of conserved nsp8 residues in its polymerase activity has so far been probed in two *in vitro* studies (Imbert et al., 2006; te Velthuis et al., 2012). In both studies, a conserved lysine (K58 in SARS-CoV) was found to be essential for polymerase activity and crucial for the binding of nsp8 to RNA (Imbert et al., 2006; te Velthuis et al., 2012). Another conserved lysine (K82) and several,

among *Coronavirinae* conserved aspartates, including a D/ExD/E motif with D50 and D52 as key residues in SARS-CoV nsp8, affected nsp8's ability to synthesize RNA *in vitro* (Imbert et al., 2006; te Velthuis et al., 2012). The critical role of the above residues was substantiated, in part, by observations that nsp8 mutations D52A and K82A cripple SARS-CoV RNA synthesis in cell culture and that mutation K58A is lethal for the virus (Subissi et al., 2014b). However, nsp8 shares no structural homology with other primases or RNA polymerases (see Section 6), so in the absence of a tertiary structure of nsp8 bound to RNA and nucleotides, it is presently unclear how these putative active site residues may assist the nucleotide condensation activity of nsp8 *in vitro* (Imbert et al., 2006; te Velthuis et al., 2012). Moreover, as for SARS-CoV nsp12, contradictory results have been obtained in the handful of nsp8 studies performed by different laboratories, which may have been due to differences in experimental design and/or the fact that nidovirus RdRps appear to be technically challenging proteins. Unfortunately, we therefore have to conclude that the question whether nsp8 functions as primase still remains wide open. In the next section, we will elaborate on the role of nsp8 as a cofactor for RNA replication by nsp12 in more detail.

6. The RNA polymerase activity of nsp12 and the role of nsp8 as co-factor: the nsp7+8+12 tripartite complex

In 2005, the SARS-CoV 22-kDa nsp8 was shown to form a ring-like complex together with the 12-kDa nsp7 (Zhai et al., 2005) (Fig. 4A–C). This complex consisted of 8 copies of each subunit, oriented such that the inner cavity of the ring was positively charged and capable of binding RNA (Zhai et al., 2005) (Fig. 4A). Given the structural similarity of this hexadecamer to the eukaryotic PCNA sliding clamp and the β-subunit of the *E. coli* DNA polymerase III, it was proposed that it could function as a processivity factor for the RNA polymerase function of nsp12 (Zhai et al., 2005). Interestingly, nsp7 and nsp8 from the distantly related feline coronavirus (FCoV) were found to form a different nsp7+8 complex in which nsp7 and nsp8 form a heterotrimer consisting of 2 copies of nsp7 and 1 copy of nsp8 (Fig. 4D) (Xiao et al., 2012). Although the heterotrimer was found to be the most likely complex in solution, it may be possible that this trimer forms higher order structures, as it can self-interact under crystallization conditions and form a heterohexamer (Xiao et al., 2012). Together with the observations from Zhai et al., this suggests that the nsp7+8 complex is relatively plastic and that it may perform multiple functions. Indeed, several nsp7+8 complexes have been observed across a number of experiments and studies (te Velthuis et al., 2012; Xiao et al., 2012; Zhai et al., 2005). Alternatively, the difference between the various nsp7+8 complex structures can be attributed to the position of the purification tags, the genetic background of the protein (FCoV versus SARS-CoV) or the crystallization procedures (Xiao et al., 2012).

In contrast to their oligomeric form, the structure of the individual nsp7 and nsp8 subunits is consistent across the structural studies. Nsp7 adopts a globular structure that consists mostly of alpha-helices, both in solution and in the nsp7+8 crystal (Johnson et al., 2010; Zhai et al., 2005). Nsp8 can adopt a golf club-like shape that is present in a 'straight' (nsp8-I) and 'bent' (nsp8-II) conformation. Both forms are present in the hexadecameric nsp7+8 complex (Fig. 4B and C), but only the 'straight' form of nsp8 is seen in the FCoV nsp7+8 complex (Xiao et al., 2012) (Fig. 4D). Inside the ring structure, SARS-CoV nsp7 and nsp8 interact extensively, with nsp7 likely stabilising the framework of interlinking nsp8 subunits (Zhai et al., 2005). Although SARS-CoV nsp8 can assemble into oligomers in the absence of nsp7 (te Velthuis et al., 2012; Zhai et al., 2005), (Johnson et al., 2010; Xiao et al., 2012; Zhai et al., 2005), nsp7+8 complexes were found to have a higher RNA binding affinity than nsp8 oligomers alone (te Velthuis et al., 2012) and mutations in nsp7 affect the RNA binding ability of the nsp7+8 complex (Subissi et al., 2014b).

In multiple earlier studies, nsp7 and nsp8 were also shown to co-purify or interact with nsp12 (Imbert et al., 2008; von Brunn et al., 2007). In 2014, Subissi et al. discovered that an unknown form of the nsp7+8 complex can interact with nsp12-strep and increase the processivity of its primer-dependent polymerase activity several orders of magnitude (Subissi et al., 2014b). In the presence of Mg^{2+}, the nsp7+8+12 tripartite complex was also able to initiate RNA synthesis *de novo* on a 339-nt long fragment representing the 3′-terminal part of the viral genome (Subissi et al., 2014b). Interestingly, the efficiency of the polymerase reaction was improved by creating a physical link between the nsp7 and nsp8 subunits in the form of a 6- or 12-amino acid linker (nsp7L8), which suggests that nsp7+8 complex formation on the template is a rate-limiting step (Subissi et al., 2014b). Subissi et al. also found that the nsp7L8+12-strep complex had a higher RNA binding affinity than nsp7L8 or nsp12-strep alone, of which the latter was unable to bind to the RNA template (Subissi et al., 2014b). Unfortunately, no direct comparison was made between nsp7+8 and nsp7L8, so it is unclear whether the nsp7+8+12-strep complex behaves in a similar fashion.

Mutagenesis of SARS-CoV nsp8 within the context of the nsp7+8+12 complex resulted in the identification of residues that are important for the interaction between nsp8 and nsp12 (nsp8 P183 and nsp8 R190). As in studies on nsp8 alone and the nsp7+8 complex, residue K58, which is fully conserved among members of the *Coronaviridae* family, was found to be involved in the binding of the RNA template. In line with their observed roles in the complex, each of these three mutations also inactivated the primer-dependent and *de novo* activity of the nsp7+8+12 complex *in vitro* and resulted in a non-viable virus phenotype when reverse-engineered into the SARS-CoV genome (Subissi et al., 2014b). By contrast to the above three mutations, only limited correlation between the biochemical and the reverse genetics data was observed for other mutations in nsp8, suggesting that the role of nsp7 and nsp8 in the RTC is more complex than the *in vitro* experiments will have us believe. Nsp8 mutants D52A or K82A, which were found to cripple the nsp7+8 activity *in vitro* (te Velthuis et al., 2012) and viral RNA synthesis in cell culture (Subissi et al., 2014b), did not affect nsp7+8+12 complex formation or the primer extension activity of the nsp7+8+12 complex. This suggests that the RdRp activity of nsp7+8 as observed by te Velthuis et al. is not involved in the primer-extension activity of the nsp7+8+12 complex, which provides support for the hypothesis that nsp7+8 acts as a processivity factor. However, the ability of nsp8 mutants D52A and D82A to support *de novo* initiation on the 3′ terminus of the viral genome in the context of the nsp7+8+12 complex has not yet been tested.

Mutagenesis of D760 in motif C of SARS-CoV nsp12 RdRp domain (Fig. 2C) resulted in an inactive complex that showed no primer-extension and, rather surprisingly, no *de novo* initiation activity on the 3′ terminus of the viral genome. In light of the previous biochemical studies on nsp8 and nsp12, it is difficult to interpret this result. On the one hand, it suggests that only nsp12 can actively catalyse RNA synthesis, while nsp7 and nsp8 are merely present as co-factors. On the other hand, it is presently just as likely that nsp12 is a dominant factor in the nsp7+8+12 complex, which regulates the primase and elongation activities of nsp8, or that nsp7+8+12 is still an incomplete or incorrectly assembled complex. In turn, the lack of one or more additional (protein or RNA) factors may prevent us from seeing consistency between the biochemical responses of the polymerase complex *in vitro* and the functionality of the RTC in the infected cell. Clearly, both the role of nsp8 (primase and/or processivity factor?) and the initiation mechanism employed by nsp12 require further study.

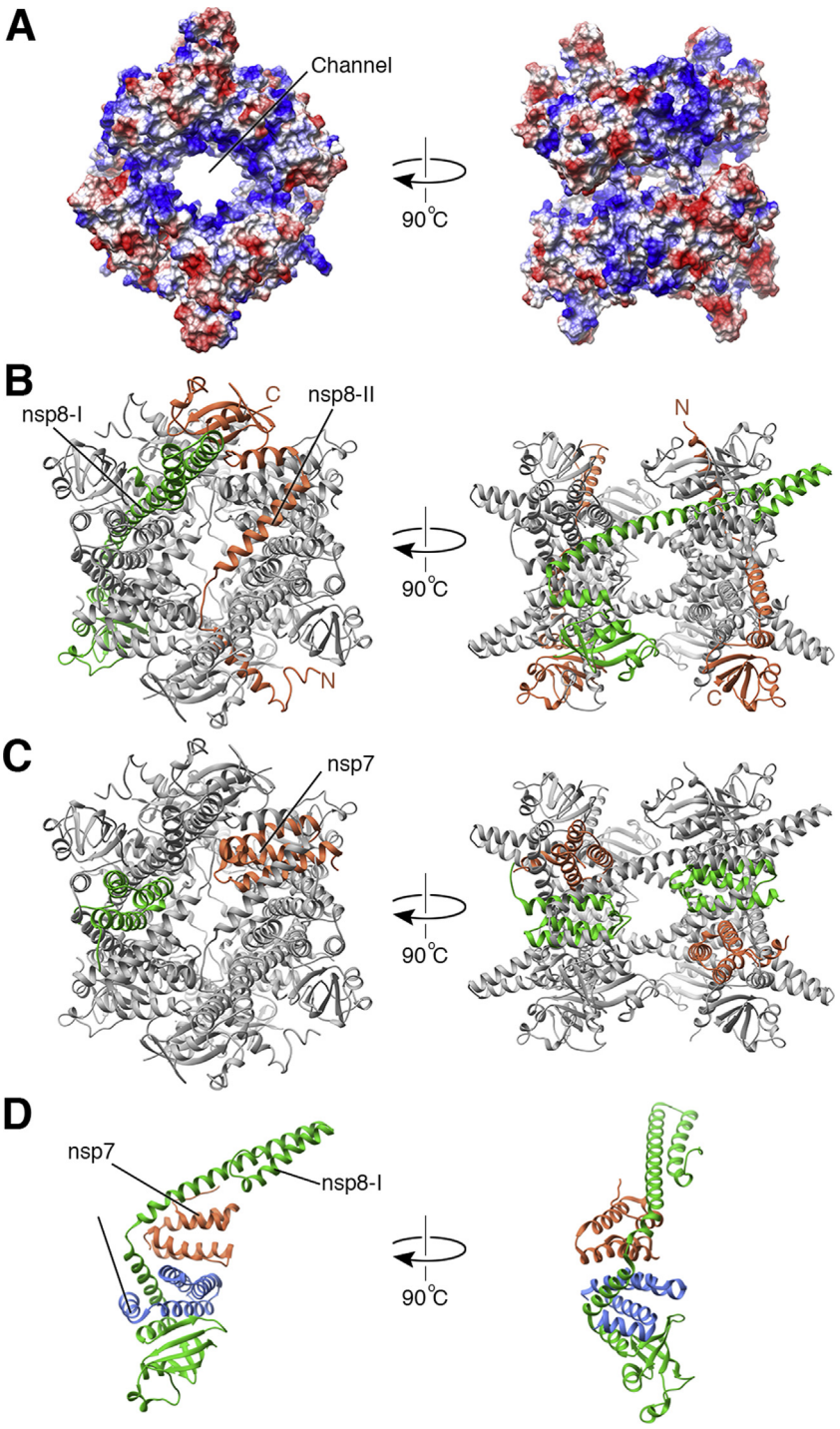

Fig. 4. The structure of the CoV nsp7-8 complex. A) The hollow hexadecameric ring of the SARS-CoV nsp7-8 complex has a positively charged channel (blue surface shading) that is likely important for RNA binding. The outside of the hexadecamer is predominantly negatively charged (red surface shading). B) The SARS-CoV nsp8 crystal structure (pdb 2AHM) resembles a 'golf club' with a long stick at the N-terminus (N) and a head-like shape at the C-terminus (C). The nsp8 structure can adopt two conformations, here shaded green (nsp8-I) and orange (nsp8-II). C) In the hexadecamer each of the two nsp8 structures is present four times and complemented by eight nsp7 subunits that act as mortar. Two orientations of the nsp7 subunit are indicated (orange and green). D) The FCOV heterotrimeric nsp7-8 complex (pdb 3ub0) consists of one nsp8 (shaded green) subunit and two nsp7 subunits (orange and blue). The nsp8 subunit adopts an nsp8-I conformation.

7. The elusive *in vitro* RNA polymerase activity of AV nsp9

To our knowledge, attempts to achieve *in vitro* activity of an AV RdRp have only been made using EAV nsp9. By contrast to SARS-CoV nsp12, recombinant EAV nsp9 with a C-terminal His-tag could be stably expressed to high levels in *E. coli* and readily purified (Beerens et al., 2007; Lehmann et al., 2016). Beerens et al. reported that recombinant EAV nsp9 is capable of *de novo* initiation of RNA synthesis on homopolymeric templates (poly(C) and poly(U)). However, no activity was found when an RNA template representing the 3′-terminal part of the viral genome was provided or when a primer was hybridized to the template (Beerens et al.,

2007). On the homopolymeric templates, RNA synthesis required the presence of Mn^{2+}, but it could be stimulated by Mg^{2+} if Mn^{2+} was present. Although no active site mutant was tested in the initial EAV nsp9 study, the *de novo* initiation on the poly(U) template was repeated in a subsequent study with a wild-type (wt) EAV nsp9 and D445A motif A mutant. In these assays, the D445A mutant showed a significantly reduced activity compared to the wt control (te Velthuis et al., 2010b). Unfortunately, more recent efforts using the same T7-driven expression construct failed to reproduce these observations regarding the activity of nsp9 (Lehmann et al., 2016). Sufficient C-terminally His_6-tagged nsp9 could be purified, but after extensive mutation of the conserved motif A and C aspartates the protein preparations continued to show *de novo* and primer-dependent polymerase activities on both RNA and DNA templates (Lehmann et al., 2016). It was thus concluded that contaminating trace amounts of T7 RNA polymerase may have produced these results. To alleviate this problem, nsp9 was expressed in a T7 polymerase-free *E. coli* system that had previously been used to express a C-terminally tagged nsp12 with a native N-terminus (te Velthuis et al., 2010a). Unfortunately, this recombinant version of nsp9 showed no *de novo* polymerase activity, while the primer-dependent and terminal transferase activities were insensitive to replacement of the conserved motif A and C aspartates (Lehmann et al., 2016). It must therefore be concluded that, as for SARS-CoV nsp12, the activity of nsp9 likely is very weak and sensitive to the purification or assay conditions, and that – by analogy with CoV nsp12 – other co-factors may be required to stimulate its activity. However, preliminary experiments in which RdRp assays with recombinant EAV nsp9 were supplemented with several small products from the nsp6-8 region of pp1a failed to activate RNA synthesis *in vitro* (Lehmann et al., 2016).

8. The nidovirus-specific domain at the N-terminus of the RdRp-containing subunit: NiRAN

It has long been recognized that the nidovirus replicase subunit that harbours the RdRp domain has an unusually large N-terminal extension that does not seem to be part of the RdRp domain itself. No viral or cellular homologues have been identified thus far, and even within the order *Nidovirales* the level of conservation of this domain is very limited, which long hampered attempts to deduce a possible function and/or activity by using bioinformatics tools. In a recent study that combined extensive bioinformatics analysis, biochemical studies and reverse genetics, a nucleotidylation activity was assigned to this domain, which was named NiRAN (Lehmann et al., 2015a). The domain is only present in nidoviruses and, in addition to a unique zinc-binding domain (ZBD) that is associated with the nidovirus helicase (Deng et al., 2014), is considered to be a second universal genetic marker for this virus order, and the first with an enzymatic activity. Despite limited sequence conservation and significant size differences, from ~220 residues in AV to over 300 residues in CoV, three motifs were identified: A_N, B_N and C_N (the subscript N for the NiRAN domain was added to discriminate them from the conserved RdRp domain motifs). Together these contain only seven residues that are absolutely conserved among nidoviruses (Fig. 2B). There is a marked size difference in the spacing between NiRAN domain motifs B_N and C_N when comparing AV with all other nidovirus lineages: these motifs are adjacent in AV, but separated by 40–60 residues in other nidoviruses. The C-terminal border of the domain could not be defined with certainty leaving room for the presence of a third domain of ~50 or ~175 amino acids for AV and CoV, respectively, that may connect the NiRAN and RdRp domains (Lehmann et al., 2015a).

Nucleotidylation activity was shown for recombinant EAV nsp9, expressed in and purified from *E. coli*. Incubation of the protein with [α-^{32}P]GTP or [α-^{32}P]UTP, but not [γ-^{32}P]-labelled nucleotides, resulted in labelling of nsp9 itself, which was attributed to the covalent binding of monophosphate nucleotides while releasing pyrophosphate (Lehmann et al., 2015a). This reaction was Mn^{2+}-dependent and displayed a 5-fold stronger affinity for UTP over GTP as a substrate. Most likely a phosphoamide bond is formed between the nucleotide and a conserved lysine in motif A_N (K54 in EAV nsp9). Mutagenesis of conserved residues in motifs A_N, B_N or C_N resulted in less than 10% *in vitro* activity for all but the K106A mutant, which confirmed the association of the nucleotidylation activity with the N-terminal domain of nsp9. A D445A mutation in motif A of the nsp9 RdRp domain only moderately affected nucleotidylation, strengthening the notion that this activity is associated with the NiRAN domain. For both EAV nsp9 and SARS-CoV nsp12, it was shown that the NiRAN domain is essential for viral replication: reverse engineered mutants with substitutions in the motifs of the NiRAN domain were either non-viable or crippled, in which case they mostly reverted back to the wt sequence (Lehmann et al., 2015a).

Despite convincing evidence for the nucleotidylation activity of EAV nsp9, this activity is yet to be demonstrated for CoVs and other members of the order *Nidovirales*. In addition, the role of this activity in the nidovirus replicative cycle remains unknown. Given its covalent linkage to the RdRp domain, it has been suggested that NiRAN is important for RNA synthesis, in analogy to the N-terminal domain of the RdRp of double-stranded RNA viruses (Tao et al., 2002; Xu et al., 2003). It may also add to the stability of the NiRAN and RdRp-containing replicase subunit, as suggested by the inability to express EAV nsp9 when the N-terminal domain is deleted (Beerens et al., 2007). While an RdRp mutation moderately influenced NiRAN nucleotidylation, it was unfortunately not possible to study the effect of NiRAN mutations on AV RNA polymerase activity, as a robust *in vitro* assay remains to be developed (see above). Yet, given the integration of the two domains in a single replicase subunit, structural and/or functional crosstalk between the NiRAN and the RdRp domain is a likely scenario.

So far, three possible functions have been proposed for the nucleotidylation activity of the NiRAN domain in nidoviral replication (Lehmann et al., 2015a). The first is a role in the ligation of yet to be identified RNA molecules based on the domain's ability to covalently bind nucleotide monophosphates, one of the steps of the universal ligation mechanism (Shuman and Lima, 2004). A second is a possible role in the 5′ capping of mRNAs, while a third possibility is that the NiRAN domain is involved in facilitating protein-primed RNA synthesis, similar to the use of a uridylated VpG primer by picornaviruses (Paul et al., 2000). Each of these hypotheses has been discussed in more detail by Lehmann et al. (2015a), but since all three require additional assumptions about nidovirus RNA synthesis they are still highly speculative. Moreover, based on the extent of divergent evolution within the NiRAN domain it cannot be excluded that the enzyme performs different roles in different nidoviruses (Lehmann et al., 2015a).

9. Faithful nidovirus replication and transcription *in vitro* and the involvement of other co-factors

The core of the nidovirus RTC likely consists of the RdRp domain-containing nsp and other viral RNA-binding proteins, like nsp7-10 and nsp13-16 in the case of CoVs. In the infected cell, these subunits assemble into a membrane-bound complex that is associated with a network of modified host membranes, presumably derived from the endoplasmic reticulum (reviewed in (Hagemeijer et al., 2012; Neuman et al., 2014; van der Hoeven et al., 2016)). An alternative approach to assay nidovirus RNA synthesis *in vitro,* without the use of purified recombinant proteins, is based on the isolation

of the membrane-associated RTCs from infected cells (van Hemert et al., 2008a, 2008b). To prepare RTCs for this *in vitro* RNA synthesis assay (IVRA), infected cells are mechanically disrupted and fractionated by centrifugation. Low speed centrifugation steps yield a post-nuclear supernatant (PNS), from which nuclei, large debris and remaining intact cells have been removed. The synthesis of SARS-CoV and EAV genome and sg mRNAs can be readily reproduced using such a PNS supplemented with [α-^{32}P]-CTP, Mg^{2+} and an ATP-generating system.

Additional fractionation of the PNS, during which the RTC-containing membranes were separated from the cytosol fraction by a high-force centrifugation step, revealed that a soluble host factor is required for CoV and AV *in vitro* RNA synthesis (van Hemert et al., 2008a, b). Further characterization of this host factor using EAV RTCs showed that it has a mass ranging from 59 to 70 kDa, that it is conserved among animals, but not lower eukaryotes, and that it can be added to inactive RTC preparations in the form of a cytosolic fraction that was extracted from uninfected cells. Presently, the exact nature of this host factor remains unknown (van Hemert et al., 2008a) and it may also not be the only host factor required for nidovirus RNA synthesis. Protein-protein (Pfefferle et al., 2011) and protein-RNA interaction studies, focusing on the 5′ and 3′ termini of the genome as putative targets (Galan et al., 2009; Spagnolo and Hogue, 2000; Tan et al., 2012), have suggested that a number of host factors, such as poly(A)-binding protein (PABP), are critical components of the CoV RTC as well. Similarly, yeast 2-hybrid (Y2H) and mammalian 2-hybrid (M2H) experiments (Imbert et al., 2008; Pan et al., 2008; Prentice et al., 2004; von Brunn et al., 2007), pull down assays or co-purifications (*e.g.* (Brockway et al., 2003; Imbert et al., 2008; Subissi et al., 2014b; Sutton et al., 2004; von Brunn et al., 2007)) and co-crystallization studies (e.g. (Decroly et al., 2011; Ma et al., 2015; Zhai et al., 2005)) have implicated several additional CoV nsps and the nucleocapsid (N) protein as potential viral co-factors of the RNA polymerase. For the AV PRRSV, using different technical approaches, multiple host proteins that appear to interact with nsp9 were identified, although it remains to be studied whether they directly bind to the RdRp domain of the protein and affect its function(s) in RNA synthesis (Dong et al., 2014; Li et al., 2014a; Liu et al., 2016). Since the exact role of these (presumed) host and viral co-factors of the nidovirus RNA polymerase remains to be explored, we will now focus on two proteins whose role in nidovirus RNA synthesis has been defined in more detail: AV nsp1 and CoV nsp14.

10. Making the RdRp switch from continuous into discontinuous mode: AV nsp1

In infected cells, the nidoviral genome and sg mRNAs are all produced with a specific relative abundance and it is poorly understood how the RNA polymerase is controlled to maintain these ratios. As outlined in the introduction, each sg mRNA is produced from a subgenome-length complement (Fig. 5), which derives from a process of discontinuous minus strand RNA synthesis (Sawicki and Sawicki, 1995; Sethna et al., 1989). Whereas continuous minus strand synthesis produces the full-length template (anti-genome) for genome replication, discontinuous minus-stranded RNA synthesis yields a nested set of shorter templates for sg mRNA production (reviewed in (Pasternak et al., 2006; Sawicki et al., 2007; Sola et al., 2011). In most nidovirus families, including AVs and CoVs, the sg mRNAs consist of sequences that are non-contiguous in the viral genome: a common 5′ 'leader' sequence is attached to different 'body' segments representing a variable part of the 3′-proximal region of the genome (Fig. 1A). The joining of leader- and body-encoding sequences occurs during discontinuous minus strand RNA synthesis (Fig. 5). Following initiation of minus strand RNA synthesis, which invariably occurs at the genomic 3′ end, a unique mechanism of 'polymerase jumping' forms the basis for leader-to-body joining. This step appears to be primarily directed by TRSs, the short conserved sequence motifs that are present in the genomic template both at the 3′ end of the leader sequence and at the 5′ end of each of the sg mRNA bodies. When minus strand RNA synthesis has been attenuated at a body TRS, the body TRS complement, which forms the 3′ end of the nascent minus strand, can base pair with the genomic leader TRS to direct re-initiation of RNA synthesis. Subsequently, the subgenome-length minus strand is completed by addition of the complement of the genomic leader sequence. The importance of (−)TRS-(+)TRS base pairing was probed and confirmed extensively by site-directed mutagenesis and reverse genetics for both AVs and CoVs (reviewed in (Pasternak et al., 2006; Sawicki et al., 2007; Sola et al., 2011). In addition to TRS base pairing, higher-order RNA structure likely co-determines the relative efficiency of different TRSs in nidovirus transcription, which mechanistically resembles the process of copy-choice RNA recombination, as it is thought to commonly occur among +RNA viruses (Pasternak et al., 2001; Sola et al., 2015; Yount et al., 2006).

The above strongly suggests that nidovirus replication and transcription are competing for common factors, like the RNA polymerase, and that the balance between continuous and discontinuous minus strand RNA synthesis must be regulated. In addition to regulatory RNA signals like the TRSs, specific replicase subunits may interact with the RNA polymerase to influence its behaviour on the genomic template. Solid support for this hypothesis was obtained in the EAV model, in particular for the nsp1 "transcription factor" and the nsp10 helicase. Specific mutations in these two subunits can (nearly) completely inactivate transcription (Nedialkova et al., 2010; Seybert et al., 2005; Tijms et al., 2001; van Dinten et al., 1997), with significant upregulation of genome replication being a prominent and striking side-effect. EAV nsp1 was concluded to control the levels at which the genome-length and different subgenome-length minus strand templates accumulate in the infected cell (Nedialkova et al., 2010). The N-terminal zinc finger domain of nsp1 is important for this function, but also mutations in other nsp1 domains can strongly influence transcription (Nedialkova et al., 2010; Tijms et al., 2001). Nsp1 mutagenesis and pseudorevertant analysis provided genetic evidence that a balanced ratio between replication and transcription, and also between individual sg mRNA species, is vital to the virus (Nedialkova et al., 2010). However, it remains unclear how AV nsp1 interacts with e.g. the network of TRS signals, the viral RNA polymerase (AV nsp9), or the helicase (AV nsp10), which has also been implicated in transcriptional control (Deng et al., 2014; Lehmann et al., 2015b). The protein could *e.g.* modulate RTC stalling at body TRSs, nascent minus strand transfer to the leader TRS or reinitiation of RNA synthesis following (−)TRS-(+)TRS base pairing. Studies aiming to detect AV nsp1-nsp9 or nsp1-nsp10 interactions have not been successful so far, but it is conceivable that such complexes are short-lived. Clearly, a robust *in vitro* AV RdRp assay could be a ground-breaking tool to explore attenuation during minus-strand RNA synthesis, TRS base pairing and the role of regulatory protein factors like AV nsp1 and nsp10.

The composition of the RNA-synthesizing complexes that other nidoviruses employ for replication and transcription has not yet been studied in great detail. Their much larger genome size than the AV genome clearly provides ample grounds to speculate that they may encode mechanisms and factors that are lacking in the AV system. Still, thus far only a few studies have suggested the existence of CoV "transcription factors" with an impact resembling that of AV nsp1. A point mutation in the helicase (nsp13) of the CoV infectious bronchitis virus was reported to cause a specific block in transcription (Fang et al., 2007), but this observation has not been followed up in more detail for any CoV thus far. More recently, N

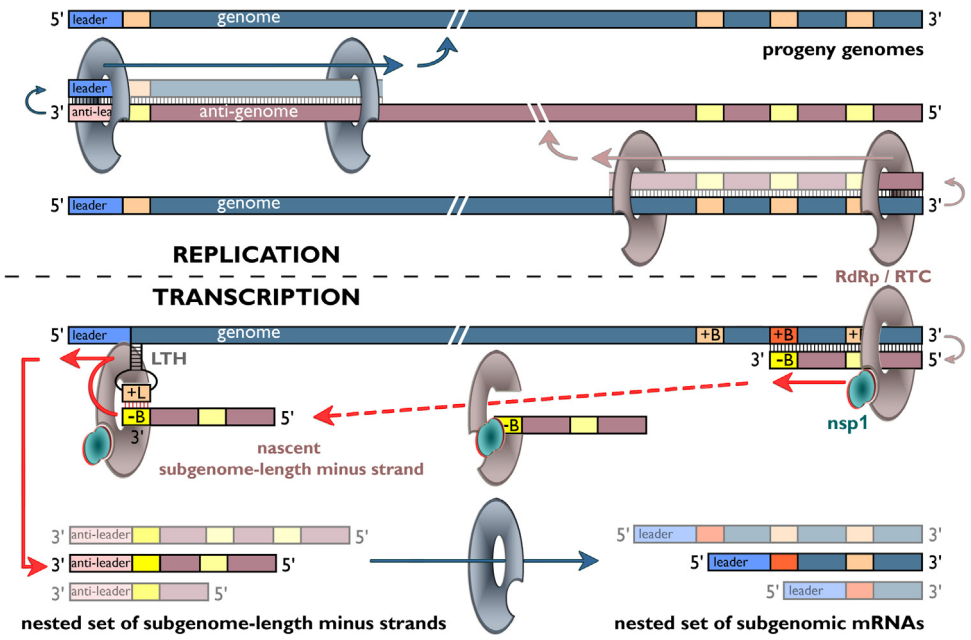

Fig. 5. Nidovirus RNA synthesis. Model for replication and transcription using a hypothetical genome encoding three sg mRNAs. The top half of the scheme depicts the replication of the genome from a full-length minus-strand intermediate (antigenome). The bottom half illustrates how minus-strand RNA synthesis can be attenuated at a body TRS (+B), after which the nascent minus strand, having a body TRS complement (−B) at its 3′ end, is redirected to the leader TRS (+L) near the 5′ end of the genome. Guided by a base-pairing interaction between the −B and +L sequences, RNA synthesis is resumed to add the anti-leader sequence to each nascent subgenome-length minus strand. Subsequently, the latter serves as template to produce a sg mRNA. The RdRp complexes engaged in replication and transcription may differ, as transcription-specific regulatory protein factors, like EAV nsp1, have been described (Nedialkova et al., 2010). For further details, see text. Adapted from (Snijder and Kikkert, 2013).

protein phosphorylation by the host kinase GSK-3 was reported to affect the relative abundance of MHV mRNAs in infected cells (Wu et al., 2014). Inhibition of GSK-3 was found to reduce the accumulation of MHV genome and longer, but not shorter, sg mRNAs, a result that could be reproduced upon the siRNA-mediated knockdown of the cellular helicase DDX1, which was found to interact with the phosphorylated form of the N protein. Recruitment of DDX1 may play a role in suppressing the attenuation of minus strand RNA synthesis at body TRSs, thus increasing the production of templates for the subsequent synthesis of the longer sg mRNAs and the viral genome. A mechanistic difference among different nidovirus lineages that has emerged is the lack of a common leader sequence in the sg mRNAs of some groups (Cowley et al., 2002; van Vliet et al., 2002). Clearly other differences may exist, but the attenuation of minus strand RNA synthesis to produce subgenome-length templates for mRNA synthesis does appear to be a conserved nidovirus feature, with a clear mechanistic connection to the processivity and other features of the RTC.

11. Polymerase fidelity and nucleotide excision by the CoV nsp14-ExoN exoribonuclease

The discovery that a CoV was the causative agent of the SARS epidemic, inspired a renewed bioinformatics analysis and led to the identification of five previously unknown RNA processing enzymes in the CoV genome (Snijder et al., 2003). One of them is a 3′-to-5′ exoribonuclease (ExoN) residing in the N-terminal domain of nsp14, which also contains a C-terminal N7-methyl transferase domain (Chen et al., 2009). This ExoN domain is present in all nidoviruses with a genome size above 20 kb (corona-, toro-, roni-, and mesoniviruses, but not arteriviruses; (Snijder et al., 2003; Lauber et al., 2012). This correlation between genome size and the presence of ExoN triggered the hypothesis that the enzyme may have been acquired to assist the RNA polymerase in achieving sufficient replication fidelity to support the unusually large genome size of the ExoN-encoding nidoviruses. By analogy with the 3′-to-5′ exonuclease domain of DNA polymerases, it was speculated that ExoN provides some kind of error correction mechanism (Snijder et al., 2003). The Mg^{2+}- or Mn^{2+}-dependent 3′-to-5′ exoribonuclease activity of recombinant SARS-CoV nsp14 could indeed be confirmed *in vitro* on double-stranded and single-stranded RNA templates (Minskaia et al., 2006). Subsequently, Bouvet et al. discovered that the *in vitro* exoribonuclease activity of nsp14 can be stimulated more than 35-fold by addition of nsp10, a small ORF1a-encoded protein that also interacts with nsp16 to enhance that subunit's 2′-*O*-methyl transferase activity, which is involved in CoV mRNA cap modification (Bouvet et al., 2012). The preferred substrates of the nsp10+14 exoribonuclease complex *in vitro* are double-stranded RNAs with or without a 3′-terminal mismatch, while RNA duplexes with longer stretches of mismatching nucleotides were found to be degraded less efficiently (Bouvet et al., 2012).

Experimental support for the hypothesis that the ExoN domain of nsp14 influences the fidelity of CoV RNA synthesis was first obtained using an MHV ExoN knockout mutant (carrying a D89A/E91A double mutation in conserved exoribonuclease motif I (Snijder et al., 2003; Zuo and Deutscher, 2001)), which was crippled but viable. This mutant displayed a mutator phenotype and – compared to the wt control – it accumulated ~15-fold more neutral mutations during serial passaging (Eckerle et al., 2007). This mutator phenotype was confirmed for SARS-CoV, with the corresponding ExoN mutant accumulating about 20 times more mutations, which were randomly distributed across the genome (Eckerle et al., 2010; Graham et al., 2012). Although these two ExoN knockout mutants replicate more slowly, they have proven to be remarkably stable (Eckerle et al., 2010; Eckerle et al., 2007). In line with the hypothesis that ExoN catalyses the excision of 3′-terminal mismatched nucleotides during RNA synthesis, the MHV ExoN knockout mutant was more sensitive to the mutagenic nucleoside analogue 5-FU (Smith et al., 2013).

The recently solved crystal structure of the SARS-CoV nsp10+14 complex revealed that nsp14 folds into two separate domains, with

residues 1–287 and 288–527 forming the N-terminal ExoN and C-terminal N7-methyl transferase domains, respectively (Ma et al., 2015). A single nsp10 molecule interacts with the ExoN domain of nsp14, which supports the available biochemical data that nsp10 only activates ribonuclease activity (Bouvet et al., 2010; Bouvet et al., 2012). Despite the presence of two unusual zinc fingers on the surface of the ExoN domain, the core structure of the enzyme is similar to that of members of the DEDD exonuclease superfamily. CoV ExoN contains five catalytic residues (D90, E92, E191, H268 and D273 in SARS-CoV), and the enzyme was classified into the subgroup of the so-called DEDDh exonucleases (Ma et al., 2015), with E191 replacing a D residue that is conserved in other members of the superfamily. A direct interaction of SARS-CoV nsp14 with nsp12 was observed in pull-down assays (Imbert et al., 2008) and the protein could also be co-purified with the nsp7+8+12 tripartite complex (Subissi et al., 2014b). This multi-nsp complex was found capable of performing all the known enzymatic activities of its subunits, *i.e.* N7-MTase, RdRp and ExoN, suggesting that the nsps involved may cooperate in the large CoV RTC during viral RNA-synthesis (Subissi et al., 2014b). Nucleotide excision by ExoN presumably occurs during RNA replication, likely following a strand transfer between the nsp12 RdRp domain and the nsp14 ExoN domain after a mismatching nucleotide has been incorporated (Bouvet et al., 2012; Subissi et al., 2014b). The structural and biochemical information obtained for nsp14 thus far provides an excellent basis to explore the function(s) and control of the unique nidoviral ExoN enzyme, and in particular its interactions with the RNA polymerase.

Given the stable viable phenotype of the ExoN domain knockout mutants in MHV and SARS-CoV, it is remarkable that similar mutants could not be recovered for two distantly related CoVs: human CoV-229E (HCoV-229E) and transmissible gastroenteritis virus (TGEV) (Becares et al., 2016; Minskaia et al., 2006). Although this may be a specific characteristic of the CoV cluster (genus alphacoronavirus) to which they belong, these findings may also reflect the complexity of the functions that nsp14 fulfills during CoV replication. In this respect, it is also noteworthy that ExoN mutations in TGEV, HCoV-229E and MHV have been reported to influence viral replication and transcription (Becares et al., 2016; Eckerle et al., 2007; Minskaia et al., 2006) and that the phenotype of ExoN knockout mutants can be strongly influenced by the innate immune response of the host cell (Becares et al., 2016).

12. Inhibitors of nidovirus RNA polymerase activity

The targeting of viral polymerases has been successfully applied as a therapeutic strategy to counter a number of DNA and RNA viruses. For RNA viruses, which generally evolve resistance mutations easily due to their high mutation frequency, polymerase inhibitors are commonly administered as part of a cocktail with drugs that target other viral or even host functions. Such combination therapies have now become the basis for the successful treatment of infections with human immunodeficiency virus and hepatitis C virus (Banerjee and Reddy, 2016; Majumdar et al., 2016; Nakamura et al., 2016; Poorolajal et al., 2016; Zeng et al., 2013).

The development of RNA polymerase inhibitors involves either the (structure-based) design of nucleoside analogues that are recognized by the polymerase and incorporated into the viral RNA genome or the screening for or designing of small molecules that inhibit nucleotide synthesis by binding to the RNA polymerase and prevent it from functioning properly. Nucleoside analogues can inhibit viral replication directly when their incorporation leads to chain termination. Alternatively, the analogue can affect viral replication indirectly by inducing so-called 'lethal mutagenesis' when the incorporation of a mutagen into nascent RNAs increases the viral mutation rate, leading to the accumulation of (too many) mutations in the viral genome, and the extinction of the virus. The inhibition of poliovirus replication by treatment with ribavirin (RBV), which is both an adenosine and guanosine analogue, is believed to mainly occur *via* the latter mechanism (Crotty et al., 2002; Crotty et al., 2001).

The combination of RBV and IFN-α2a or IFN-β1a is one of the experimental treatment options for MERS patients, despite disappointing results obtained with RBV treatment during the SARS epidemic in 2003–2004 (Lau et al., 2009). As in SARS patients, high mortality rates in comparison with untreated patients are also reported for MERS patients, but the study outcomes are difficult to compare due to significant differences in study design (for a review, see (Mo and Fisher, 2016)). *In vitro* and in small animal models, however, RBV in combination with IFN has been shown to inhibit MERS-CoV infection (Chan et al., 2015; Falzarano et al., 2013a; Falzarano et al., 2013b). The inhibition of CoV replication in cell culture by RBV alone has been investigated repeatedly for SARS-CoV, MERS-CoV and other CoVs (FCoV, PEDV) and was found to be highly variable (Chen et al., 2004; Chu et al., 2004; Cinatl et al., 2003; Hart et al., 2014; Lee et al., 2015; Morgenstern et al., 2005; Stroher et al., 2004; Tan et al., 2004; Weiss and Oostrom-Ram, 1989). The results of these cell culture-based studies need to be interpreted with caution as the uptake of RBV by several cell lines, including the frequently used African green monkey kidney (Vero) cells, is known to be inefficient (Ibarra and Pfeiffer, 2009; Shah et al., 2010). Furthermore, other mechanisms of virus inhibition by RBV have been reported that do not involve the direct targeting of the virus by incorporation of triphosphorylated RBV into nascent RNA (Beaucourt and Vignuzzi, 2014). Recently it was shown that decreased CoV replication mainly results from inhibition of inosine-5′-monophosphate dehydrogenase (IMPDH) by ribavirin monophosphate and the subsequent lowering of cellular GTP pools (Kim and Lee, 2013; Smith et al., 2014). This mechanism of action may also explain the inhibition of AV (PRRSV) replication by RBV treatment, which was not accompanied by an increased mutation frequency (Kim and Lee, 2013). In summary, it remains questionable if the incorporation of RBV-triphosphate is the mechanism of action for the inhibition of the nidovirus replication.

In the case of CoVs, also the nucleotide excision activity of the nsp14 ExoN domain may contribute to the insensitivity of viral RNA synthesis to mutagenic nucleotide analogues, provided that the ExoN domain can detect the subtle chemical differences between these compounds and regular NTPs. In line with this hypothesis, inactivation of MHV and SARS-CoV ExoN activity dramatically increased (up to 300-fold) the sensitivity to the mutagen 5-FU (Smith et al., 2013). Deep sequencing of RNA produced by wt SARS-CoV in the presence of 5-FU revealed an increase in the frequency of mutagen-associated A-to-G and U-to-C transitions, indicating that 5-FU-monophosphate was incorporated into the viral genome even in the presence of ExoN activity. However, such mutations were more frequently found in the RNA produced under similar conditions by an ExoN knockout mutant (Smith et al., 2013). The observation that even the wt virus incorporates 5-FU is consistent with the finding that nsp12 RdRp domain mutations (see above) can improve the selectivity of the viral RNA polymerase for 5-FU incorporation (Sexton et al., 2016).

Although the nsp14 ExoN activity may interfere with the effectiveness of using nucleoside analogues to inhibit CoV RNA synthesis, recently three such compounds were reported to inhibit CoV replication. Two of these were originally identified as filovirus RdRp inhibitors, but were found to display broad-spectrum activity against a range of RNA viruses including CoVs. The adenosine analogue BCX4430 inhibits CoV-induced cell death with an EC_{50} (half maximal effective concentration) of 58 and 68 μM for MERS- and SARS-CoV, respectively (Warren et al., 2014), whereas GS-5734, an

adenosine monophosphate analogue, proved to be strikingly efficient at inhibiting MERS-CoV replication with an EC_{50} of 0.34 μM (Warren et al., 2016). The third compound with anti-CoV activity is a so-called flexible purine base analogue (fleximer), combined with the acyclic sugar moiety of acyclovir, which was capable of inhibiting HCoV-NL63 and MERS-CoV (but not SARS-CoV) replication with EC_{50} values of 9 and 23–25 μM, respectively, while acyclovir was inactive (Peters et al., 2015).

The IVRA, as developed for SARS-CoV and EAV and described above, may prove to be an alternative approach to probe the mechanism of action of polymerase inhibitors. For example, using these assays, Zn^{2+} was previously identified as an inhibitor of RNA synthesis for both viruses, presumably by interfering with initiation (EAV) or elongation (SARS-CoV) (te Velthuis et al., 2010b).

In conclusion, a number of nucleoside analogues have been reported to be able to inhibit CoV replication in cell culture. However, evidence that any of these targets the CoV polymerase directly is still lacking, as biochemical assays with purified nsp12 and the triphosphate versions of these compounds remain to be performed. In addition, none of these inhibitors has been tested in animal experiments or moved forward to preclinical development. Clearly, more details on the structure and function of the CoV polymerase could accelerate the development of this type of anti-CoV drugs, which should definitely be part of our first line of defense against emerging CoV infections.

13. Conclusion and outlook

The order *Nidovirales* includes a number of important human and animal pathogens, some of which have caused considerable societal unrest and economic damage over the past decades. Unraveling how these important RNA viruses replicate and transcribe their genome is crucial for understanding nidovirus biology and the discovery of drugs for the prevention or treatment of nidovirus infections. Dissecting nidovirus RNA synthesis means unraveling the structure and function of the viral RTC and its core enzyme, the RNA polymerase. Nidovirus RTCs must handle and replicate exceptionally large RNA genomes and secure the production of a set of sg mRNAs, which are needed for the expression of their structural and accessory proteins. Possibly because of this complexity, the nidovirus RdRp-encoding subunit possesses unique features, like the presence of the N-terminally linked NiRAN domain with nucleotidylation activity. Overall, however, the nidovirus RTC, which is associated with modified intracellular membranes, is poorly understood nor do we know its exact composition in terms of viral and host components.

So far, attempts to develop *in vitro* assays using purified recombinant polymerases have produced largely contradictory results for both EAV and SARS-CoV, the only two nidoviruses for which experimental data is currently available. The addition of other nsps as co-factors (nsp7 and nsp8) in the *in vitro* CoV polymerase assays appears to offer a promising avenue for further studies and, eventually, assays for inhibitor screening. Besides the further development of robust *in vitro* polymerase assays, preferable also for the AV polymerase, several key questions remain to be answered, including (i) how do nidovirus RNA polymerases initiate RNA synthesis?; (ii) how do the ExoN and RdRp domains work together to promote polymerase fidelity?; (iii) what is the function of the conserved NiRAN domain? (iv) how is the switch from transcription to replication controlled at the molecular level?; and (v) what is the composition and structure of the RTC? In addition, three steps in the nidovirus replication cycle require the viral genome as a template: the translation of the replicase gene, the synthesis of the antigenome (template for replication) and the production of a set of subgenome-length minus strands (templates for transcription). In order to successfully produce new infectious virus particles, these events need to be coordinated and must be tightly regulated. Some regulation may be spatial (replication *vs* translation), other forms of regulation are most likely determined by specific RNA sequences and/or the conformation of the 5′- and 3′-terminal sequences of the viral RNA. How these signals affect the activity of the RNA polymerase and other RTC subunits merits further investigation.

A full understanding of the mechanisms underlying the faithful replication of the nidovirus genome will prove valuable given the unique position nidoviruses occupy in the RNA virus world. This information will deepen our understanding of the evolutionary process that has produced these unusually complex RNA virus genomes, and may aid in finding ways to combat current and future emerging nidovirus infections.

Acknowledgements

This work was supported by grant 098721/Z/12/Z from the Wellcome Trust (to A.t.V.), and TOP-GO grant 700.10.352 from the Netherlands Organization for Scientific Research (to C.C.P and E.J.S.)

References

Ahn, D.G., Choi, J.K., Taylor, D.R., Oh, J.W., 2012. Biochemical characterization of a recombinant SARS coronavirus nsp12 RNA-dependent RNA polymerase capable of copying viral RNA templates. Arch. Virol. 157, 2095–2104.
Alphonse, S., Ghose, R., 2017. Cystoviral RNA-directed RNA polymerases: regulation of RNA synthesis on multiple time and length scales. Virus Res. 234, 135–152.
Banerjee, D., Reddy, K.R., 2016. Review article: safety and tolerability of direct-acting anti-viral agents in the new era of hepatitis C therapy. Aliment. Pharmacol. Ther. 43, 674–696.
Beaucourt, S., Vignuzzi, M., 2014. Ribavirin: a drug active against many viruses with multiple effects on virus replication and propagation. Molecular basis of ribavirin resistance. Curr. Opin. Virol. 8, 10–15.
Becares, M., Pascual-Iglesias, A., Nogales, A., Sola, I., Enjuanes, L., Zuniga, S., 2016. Mutagenesis of Coronavirus nsp14 reveals its potential role in modulation of the innate immune response. J. Virol. 90, 5399–5414.
Beerens, N., Selisko, B., Ricagno, S., Imbert, I., van der Zanden, L., Snijder, E.J., Canard, B., 2007. De novo initiation of RNA synthesis by the arterivirus RNA-dependent RNA polymerase. J. Virol. 81, 8384–8395.
Biasini, M., Bienert, S., Waterhouse, A., Arnold, K., Studer, G., Schmidt, T., Kiefer, F., Gallo Cassarino, T., Bertoni, M., Bordoli, L., Schwede, T., 2014. SWISS-MODEL: modelling protein tertiary and quaternary structure using evolutionary information. Nucleic Acids Res. 42, W252–258.
Bouvet, M., Debarnot, C., Imbert, I., Selisko, B., Snijder, E.J., Canard, B., Decroly, E., 2010. In vitro reconstitution of SARS-coronavirus mRNA cap methylation. PLoS Pathog. 6, e1000863.
Bouvet, M., Imbert, I., Subissi, L., Gluais, L., Canard, B., Decroly, E., 2012. RNA 3'-end mismatch excision by the severe acute respiratory syndrome coronavirus nonstructural protein nsp10/nsp14 exoribonuclease complex. Proc. Natl. Acad. Sci. U. S. A. 109, 9372–9377.
Brockway, S.M., Clay, C.T., Lu, X.T., Denison, M.R., 2003. Characterization of the expression, intracellular localization, and replication complex association of the putative mouse hepatitis virus RNA-dependent RNA polymerase. J. Virol. 77, 10515–10527.
Castro, C., Smidansky, E.D., Arnold, J.J., Maksimchuk, K.R., Moustafa, I., Uchida, A., Gotte, M., Konigsberg, W., Cameron, C.E., 2009. Nucleic acid polymerases use a general acid for nucleotidyl transfer. Nat. Struct. Mol. Biol. 16, 212–218.
Chan, J.F., Yao, Y., Yeung, M.L., Deng, W., Bao, L., Jia, L., Li, F., Xiao, C., Gao, H., Yu, P., Cai, J.P., Chu, H., Zhou, J., Chen, H., Qin, C., Yuen, K.Y., 2015. Treatment with Lopinavir/Ritonavir or interferon-beta1b improves outcome of MERS-CoV infection in a nonhuman primate model of common marmoset. J. Infect. Dis. 212, 1904–1913.
Chen, F., Chan, K.H., Jiang, Y., Kao, R.Y., Lu, H.T., Fan, K.W., Cheng, V.C., Tsui, W.H., Hung, I.F., Lee, T.S., Guan, Y., Peiris, J.S., Yuen, K.Y., 2004. In vitro susceptibility of 10 clinical isolates of SARS coronavirus to selected antiviral compounds. J. Clin. Virol. 31, 69–75.
Chen, Y., Cai, H., Pan, J., Xiang, N., Tien, P., Ahola, T., Guo, D., 2009. Functional screen reveals SARS coronavirus nonstructural protein nsp14 as a novel cap N7 methyltransferase. Proc. Natl. Acad. Sci. U. S. A. 106, 3484–3489.
Cheng, A., Zhang, W., Xie, Y., Jiang, W., Arnold, E., Sarafianos, S.G., Ding, J., 2005. Expression, purification, and characterization of SARS coronavirus RNA polymerase. Virology 335, 165–176.
Choudhury, B., Dastjerdi, A., Doyle, N., Frossard, J.P., Steinbach, F., 2016. From the field to the lab – An European view on the global spread of PEDV. Virus Res. 226, 40–49.
Chu, C.M., Cheng, V.C., Hung, I.F., Wong, M.M., Chan, K.H., Chan, K.S., Kao, R.Y., Poon, L.L., Wong, C.L., Guan, Y., Peiris, J.S., Yuen, K.Y., Group, H.U.S.S., 2004. Role

of lopinavir/ritonavir in the treatment of SARS: initial virological and clinical findings. Thorax 59, 252–256.
Cinatl, J., Morgenstern, B., Bauer, G., Chandra, P., Rabenau, H., Doerr, H.W., 2003. Glycyrrhizin, an active component of liquorice roots, and replication of SARS-associated coronavirus. Lancet 361, 2045–2046.
Cowley, J.A., Dimmock, C.M., Walker, P.J., 2002. Gill-associated nidovirus of Penaeus monodon prawns transcribes 3'-coterminal subgenomic mRNAs that do not possess 5'-leader sequences. J. Gen. Virol. 83, 927–935.
Crotty, S., Cameron, C.E., Andino, R., 2001. RNA virus error catastrophe: direct molecular test by using ribavirin. Proc. Natl. Acad. Sci. U. S. A. 98, 6895–6900.
Crotty, S., Cameron, C.E., Andino, R., 2002. Ribavirin's antiviral mechanism of action: lethal mutagenesis? J. Mol. Med. (Berl.) 80, 86–95.
de Groot, R.J., Cowley, J.A., Enjuanes, L., Faaberg, K.S., Perlman, S., Rottier, P.J.M., Snijder, E.J., Ziebuhr, J., Gorbalenya, A.E., 2012. Order *Nidovirales*. In: King, A.M.Q., Adams, M.J., Carstens, E.B., Lefkowitz, E.J. (Eds.), Virus Taxonomy. Elsevier, Amsterdam, pp. 785–795.
den Boon, J.A., Snijder, E.J., Chirnside, E.D., de Vries, A.A., Horzinek, M.C., Spaan, W.J., 1991. Equine arteritis virus is not a togavirus but belongs to the coronaviruslike superfamily. J. Virol. 65, 2910–2920.
Decroly, E., Debarnot, C., Ferron, F., Bouvet, M., Coutard, B., Imbert, I., Gluais, L., Papageorgiou, N., Sharff, A., Bricogne, G., Ortiz-Lombardia, M., Lescar, J., Canard, B., 2011. Crystal structure and functional analysis of the SARS-coronavirus RNA cap 2'-O-methyltransferase nsp10/nsp16 complex. PLoS Pathog. 7, e1002059.
Deng, Z., Lehmann, K.C., Li, X., Feng, C., Wang, G., Zhang, Q., Qi, X., Yu, L., Zhang, X., Feng, W., Wu, W., Gong, P., Tao, Y., Posthuma, C.C., Snijder, E.J., Gorbalenya, A.E., Chen, Z., 2014. Structural basis for the regulatory function of a complex zinc-binding domain in a replicative arterivirus helicase resembling a nonsense-mediated mRNA decay helicase. Nucleic Acids Res. 42, 3464–3477.
Dong, J., Zhang, N., Ge, X., Zhou, L., Guo, X., Yang, H., 2014. The interaction of nonstructural protein 9 with retinoblastoma protein benefits the replication of genotype 2 porcine reproductive and respiratory syndrome virus in vitro. Virology 464–465, 432–440.
Dufour, D., Mateos-Gomez, P.A., Enjuanes, L., Gallego, J., Sola, I., 2011. Structure and functional relevance of a transcription-regulating sequence involved in coronavirus discontinuous RNA synthesis. J. Virol. 85, 4963–4973.
Eckerle, L.D., Lu, X., Sperry, S.M., Choi, L., Denison, M.R., 2007. High fidelity of murine hepatitis virus replication is decreased in nsp14 exoribonuclease mutants. J. Virol. 81, 12135–12144.
Eckerle, L.D., Becker, M.M., Halpin, R.A., Li, K., Venter, E., Lu, X., Scherbakova, S., Graham, R.L., Baric, R.S., Stockwell, T.B., Spiro, D.J., Denison, M.R., 2010. Infidelity of SARS-CoV Nsp14-exonuclease mutant virus replication is revealed by complete genome sequencing. PLoS Pathog. 6, e1000896.
Falzarano, D., de Wit, E., Martellaro, C., Callison, J., Munster, V.J., Feldmann, H., 2013a. Inhibition of novel beta coronavirus replication by a combination of interferon-alpha2b and ribavirin. Sci. Rep. 3, 1686.
Falzarano, D., de Wit, E., Rasmussen, A.L., Feldmann, F., Okumura, A., Scott, D.P., Brining, D., Bushmaker, T., Martellaro, C., Baseler, L., Benecke, A.G., Katze, M.G., Munster, V.J., Feldmann, H., 2013b. Treatment with interferon-alpha2b and ribavirin improves outcome in MERS-CoV-infected rhesus macaques. Nat. Med. 19, 1313–1317.
Fang, S., Chen, B., Tay, F.P., Ng, B.S., Liu, D.X., 2007. An arginine-to-proline mutation in a domain with undefined functions within the helicase protein (Nsp13) is lethal to the coronavirus infectious bronchitis virus in cultured cells. Virology 358, 136–147.
Fang, Y., Treffers, E.E., Li, Y., Tas, A., Sun, Z., van der Meer, Y., de Ru, A.H., van Veelen, P.A., Atkins, J.F., Snijder, E.J., Firth, A.E., 2012. Efficient −2 frameshifting by mammalian ribosomes to synthesize an additional arterivirus protein. Proc. Natl. Acad. Sci. U. S. A. 109, E2920–2928.
Galan, C., Sola, I., Nogales, A., Thomas, B., Akoulitchev, A., Enjuanes, L., Almazan, F., 2009. Host cell proteins interacting with the 3' end of TGEV coronavirus genome influence virus replication. Virology 391, 304–314.
Gorbalenya, A.E., Koonin, E.V., Donchenko, A.P., Blinov, V.M., 1989. Coronavirus genome: prediction of putative functional domains in the non-structural polyprotein by comparative amino acid sequence analysis. Nucleic Acids Res. 17, 4847–4861.
Gorbalenya, A.E., Pringle, F.M., Zeddam, J.L., Luke, B.T., Cameron, C.E., Kalmakoff, J., Hanzlik, T.N., Gordon, K.H., Ward, V.K., 2002. The palm subdomain-based active site is internally permuted in viral RNA-dependent RNA polymerases of an ancient lineage. J. Mol. Biol. 324, 47–62.
Gorbalenya, A.E., Enjuanes, L., Ziebuhr, J., Snijder, E.J., 2006. Nidovirales: evolving the largest RNA virus genome. Virus Res. 117, 17–37.
Graham, R.L., Becker, M.M., Eckerle, L.D., Bolles, M., Denison, M.R., Baric, R.S., 2012. A live, impaired-fidelity coronavirus vaccine protects in an aged, immunocompromised mouse model of lethal disease. Nat. Med. 18, 1820–1826.
Graham, R.L., Donaldson, E.F., Baric, R.S., 2013. A decade after SARS: strategies for controlling emerging coronaviruses. Nat. Rev. Microbiol. 11, 836–848.
Hagemeijer, M.C., Rottier, P.J., de Haan, C.A., 2012. Biogenesis and dynamics of the coronavirus replicative structures. Viruses 4, 3245–3269.
Hart, B.J., Dyall, J., Postnikova, E., Zhou, H., Kindrachuk, J., Johnson, R.F., Olinger Jr., G.G., Frieman, M.B., Holbrook, M.R., Jahrling, P.B., Hensley, L., 2014. Interferon-beta and mycophenolic acid are potent inhibitors of Middle East respiratory syndrome coronavirus in cell-based assays. J. Gen. Virol. 95, 571–577.
Holtkamp, D.J., Kliebenstein, J.B., Neumann, E.J., Zimmerman, J.J., Rotto, H.F., Yoder, T.K., Wang, C., Yeske, P.E., Mowrer, C.L., Haley, C.A., 2013. Assessment of the economic impact of porcine reproductive and respiratory syndrome virus on United States pork producers. J. Swine Health Prod. 21, 72–84.
Ibarra, K.D., Pfeiffer, J.K., 2009. Reduced ribavirin antiviral efficacy via nucleoside transporter-mediated drug resistance. J. Virol. 83, 4538–4547.
Imbert, I., Guillemot, J.C., Bourhis, J.M., Bussetta, C., Coutard, B., Egloff, M.P., Ferron, F., Gorbalenya, A.E., Canard, B., 2006. A second, non-canonical RNA-dependent RNA polymerase in SARS coronavirus. EMBO J. 25, 4933–4942.
Imbert, I., Snijder, E.J., Dimitrova, M., Guillemot, J.C., Lecine, P., Canard, B., 2008. The SARS-Coronavirus PLnc domain of nsp3 as a replication/transcription scaffolding protein. Virus Res. 133, 136–148.
Johnson, M.A., Jaudzems, K., Wuthrich, K., 2010. NMR structure of the SARS-CoV nonstructural protein 7 in solution at pH 6.5. J. Mol. Biol. 402, 619–628.
Kelley, L.A., Mezulis, S., Yates, C.M., Wass, M.N., Sternberg, M.J., 2015. The Phyre2 web portal for protein modeling, prediction and analysis. Nat. Protoc. 10, 845–858.
Kim, Y., Lee, C., 2013. Ribavirin efficiently suppresses porcine nidovirus replication. Virus Res. 171, 44–53.
Lau, E.H., Cowling, B.J., Muller, M.P., Ho, L.M., Tsang, T., Lo, S.V., Louie, M., Leung, G.M., 2009. Effectiveness of ribavirin and corticosteroids for severe acute respiratory syndrome. Am. J. Med. 122 (115), e1111–1121.
Lauber, C., Ziebuhr, J., Junglen, S., Drosten, C., Zirkel, F., Nga, P.T., Morita, K., Snijder, E.J., Gorbalenya, A.E., 2012. Mesoniviridae: a proposed new family in the order Nidovirales formed by a single species of mosquito-borne viruses. Arch. Virol. 157, 1623–1628.
Lauber, C., Goeman, J.J., Parquet Mdel, C., Nga, P.T., Snijder, E.J., Morita, K., Gorbalenya, A.E., 2013. The footprint of genome architecture in the largest genome expansion in RNA viruses. PLoS Pathog. 9, e1003500.
Lee, J.H., Park, J.S., Lee, S.W., Hwang, S.Y., Young, B.E., Choi, H.J., 2015. Porcine epidemic diarrhea virus infection: inhibition by polysaccharide from Ginkgo biloba exocarp and mode of its action. Virus Res. 195, 148–152.
Lehmann, K.C., Gulyaeva, A., Zevenhoven-Dobbe, J.C., Janssen, G.M., Ruben, M., Overkleeft, H.S., van Veelen, P.A., Samborskiy, D.V., Kravchenko, A.A., Leontovich, A.M., Sidorov, I.A., Snijder, E.J., Posthuma, C.C., Gorbalenya, A.E., 2015a. Discovery of an essential nucleotidylating activity associated with a newly delineated conserved domain in the RNA polymerase-containing protein of all nidoviruses. Nucleic Acids Res. 43, 8416–8434.
Lehmann, K.C., Snijder, E.J., Posthuma, C.C., Gorbalenya, A.E., 2015b. What we know but do not understand about nidovirus helicases. Virus Res. 202, 12–32.
Lehmann, K.C., Gorbalenya, A.E., Snijder, E.J., Posthuma, C.C., 2016. Arterivirus RNA-dependent RNA polymerase: vital enzymatic activity remains elusive. Virology 487, 68–74.
Li, J., Guo, D., Huang, L., Yin, M., Liu, Q., Wang, Y., Yang, C., Liu, Y., Zhang, L., Tian, Z., Cai, X., Yu, L., Weng, C., 2014a. The interaction between host Annexin A2 and viral Nsp9 is beneficial for replication of porcine reproductive and respiratory syndrome virus. Virus Res. 189, 106–113.
Li, Y., Treffers, E.E., Napthine, S., Tas, A., Zhu, L., Sun, Z., Bell, S., Mark, B.L., van Veelen, P.A., van Hemert, M.J., Firth, A.E., Brierley, I., Snijder, E.J., Fang, Y., 2014b. Transactivation of programmed ribosomal frameshifting by a viral protein. Proc. Natl. Acad. Sci. U. S. A. 111, E2172–2181.
Liu, D.X., Fung, T.S., Chong, K.K., Shukla, A., Hilgenfeld, R., 2014. Accessory proteins of SARS-CoV and other coronaviruses. Antiviral Res. 109, 97–109.
Liu, L., Tian, J., Nan, H., Tian, M., Li, Y., Xu, X., Huang, B., Zhou, E., Hiscox, J.A., Chen, H., 2016. Porcine reproductive and respiratory syndrome virus nucleocapsid protein interacts with nsp9 and cellular DHX9 to regulate viral RNA synthesis. J. Virol. 90, 5384–5398.
Ma, Y., Wu, L., Shaw, N., Gao, Y., Wang, J., Sun, Y., Lou, Z., Yan, L., Zhang, R., Rao, Z., 2015. Structural basis and functional analysis of the SARS coronavirus nsp14-nsp10 complex. Proc. Natl. Acad. Sci. U. S. A. 112, 9436–9441.
Madhugiri, R., Fricke, M., Marz, M., Ziebuhr, J., 2016. Coronavirus cis-acting RNA elements. Adv. Virus Res. 96, 127–163.
Majumdar, A., Kitson, M.T., Roberts, S.K., 2016. Systematic review: current concepts and challenges for the direct-acting antiviral era in hepatitis C cirrhosis. Aliment. Pharmacol. Ther. 43, 1276–1292.
Masters, P.S., 2007. Genomic cis-acting elements in coronavirus RNA replication. In: Thiel, V. (Ed.), Coronaviruses—Molecular and Cellular Biology. Caister Academic Press, Norfolk, UK, pp. 65–80.
Menachery, V.D., Yount Jr., B.L., Debbink, K., Agnihothram, S., Gralinski, L.E., Plante, J.A., Graham, R.L., Scobey, T., Ge, X.Y., Donaldson, E.F., Randell, S.H., Lanzavecchia, A., Marasco, W.A., Shi, Z.L., Baric, R.S., 2015. A SARS-like cluster of circulating bat coronaviruses shows potential for human emergence. Nat. Med. 21, 1508–1513.
Minskaia, E., Hertzig, T., Gorbalenya, A.E., Campanacci, V., Cambillau, C., Canard, B., Ziebuhr, J., 2006. Discovery of an RNA virus 3'- > 5' exoribonuclease that is critically involved in coronavirus RNA synthesis. Proc. Natl. Acad. Sci. U. S. A. 103, 5108–5113.
Mo, Y., Fisher, D., 2016. A review of treatment modalities for middle east respiratory syndrome. J. Antimicrob. Chemother. 71, 3340–3350.
Morgenstern, B., Michaelis, M., Baer, P.C., Doerr, H.W., Cinatl Jr., J., 2005. Ribavirin and interferon-beta synergistically inhibit SARS-associated coronavirus replication in animal and human cell lines. Biochem. Biophys. Res. Commun. 326, 905–908.
Nakamura, M., Kanda, T., Haga, Y., Sasaki, R., Wu, S., Nakamoto, S., Yasui, S., Arai, M., Imazeki, F., Yokosuka, O., 2016. Sofosbuvir treatment and hepatitis C virus infection. World J. Hepatol. 8, 183–190.

Nedialkova, D.D., Gorbalenya, A.E., Snijder, E.J., 2010. Arterivirus Nsp1 modulates the accumulation of minus-strand templates to control the relative abundance of viral mRNAs. PLoS Pathog. 6, e1000772.
Neuman, B.W., Chamberlain, P., Bowden, F., Joseph, J., 2014. Atlas of coronavirus replicase structure. Virus Res. 194, 49–66.
Pan, J., Peng, X., Gao, Y., Li, Z., Lu, X., Chen, Y., Ishaq, M., Liu, D., Dediego, M.L., Enjuanes, L., Guo, D., 2008. Genome-wide analysis of protein–protein interactions and involvement of viral proteins in SARS-CoV replication. PLoS One 3, e3299.
Pasternak, A.O., van den Born, E., Spaan, W.J., Snijder, E.J., 2001. Sequence requirements for RNA strand transfer during nidovirus discontinuous subgenomic RNA synthesis. EMBO J. 20, 7220–7228.
Pasternak, A.O., Spaan, W.J., Snijder, E.J., 2006. Nidovirus transcription: how to make sense.? J. Gen. Virol. 87, 1403–1421.
Paul, A.V., Rieder, E., Kim, D.W., van Boom, J.H., Wimmer, E., 2000. Identification of an RNA hairpin in poliovirus RNA that serves as the primary template in the in vitro uridylylation of VPg. J. Virol. 74, 10359–10370.
Perez, A.M., Davies, P.R., Goodell, C.K., Holtkamp, D.J., Mondaca-Fernandez, E., Poljak, Z., Tousignant, S.J., Valdes-Donoso, P., Zimmerman, J.J., Morrison, R.B., 2015. Lessons learned and knowledge gaps about the epidemiology and control of porcine reproductive and respiratory syndrome virus in North America. J. Am. Vet. Med. Assoc. 246, 1304–1317.
Perlman, S., Netland, J., 2009. Coronaviruses post-SARS: update on replication and pathogenesis. Nat. Rev. Microbiol. 7, 439–450.
Peters, H.L., Jochmans, D., de Wilde, A.H., Posthuma, C.C., Snijder, E.J., Neyts, J., Seley-Radtke, K.L., 2015. Design, synthesis and evaluation of a series of acyclic fleximer nucleoside analogues with anti-coronavirus activity. Bioorg. Med. Chem. Lett. 25, 2923–2926.
Pfefferle, S., Schopf, J., Kogl, M., Friedel, C.C., Muller, M.A., Carbajo-Lozoya, J., Stellberger, T., von Dall'Armi, E., Herzog, P., Kallies, S., Niemeyer, D., Ditt, V., Kuri, T., Zust, R., Pumpor, K., Hilgenfeld, R., Schwarz, F., Zimmer, R., Steffen, I., Weber, F., Thiel, V., Herrler, G., Thiel, H.J., Schwegmann-Wessels, C., Pohlmann, S., Haas, J., Drosten, C., von Brunn, A., 2011. The SARS-coronavirus-host interactome: identification of cyclophilins as target for pan-coronavirus inhibitors. PLoS Pathog. 7, e1002331.
Pflug, A., Lukarska, M., Resa-Infante, P., Reich, S., 2017. Structural insights into RNA synthesis by the influenza virus transcription-replication machine. Virus Res. 234, 103–117.
Pileri, E., Mateu, E., 2016. Review on the transmission porcine reproductive and respiratory syndrome virus between pigs and farms and impact on vaccination. Vet. Res. 47, 108.
Poch, O., Sauvaget, I., Delarue, M., Tordo, N., 1989. Identification of four conserved motifs among the RNA-dependent polymerase encoding elements. EMBO J. 8, 3867–3874.
Poorolajal, J., Hooshmand, E., Mahjub, H., Esmailnasab, N., Jenabi, E., 2016. Survival rate of AIDS disease and mortality in HIV-infected patients: a meta-analysis. Public Health 139, 3–12.
Prentice, E., Jerome, W.G., Yoshimori, T., Mizushima, N., Denison, M.R., 2004. Coronavirus replication complex formation utilizes components of cellular autophagy. J. Biol. Chem. 279, 10136–10141.
Reguera, J., Gerlach, P., Cusack, S., 2016. Towards a structural understanding of RNA synthesis by negative strand RNA viral polymerases. Curr. Opin. Struct. Biol. 36, 75–84.
Sawicki, S.G., Sawicki, D.L., 1995. Coronaviruses use discontinuous extension for synthesis of subgenome-length negative strands. Adv. Exp. Med. Biol. 380, 499–506.
Sawicki, S.G., Sawicki, D.L., Siddell, S.G., 2007. A contemporary view of coronavirus transcription. J. Virol. 81, 20–29.
Sethna, P.B., Hung, S.L., Brian, D.A., 1989. Coronavirus subgenomic minus-strand RNAs and the potential for mRNA replicons. Proc. Natl. Acad. Sci. U. S. A. 86, 5626–5630.
Sexton, N.R., Smith, E.C., Blanc, H., Vignuzzi, M., Peersen, O.B., Denison, M.R., 2016. Homology-Based identification of a mutation in the Coronavirus RNA-dependent RNA polymerase that confers resistance to multiple mutagens. J. Virol. 90, 7415–7428.
Seybert, A., Posthuma, C.C., van Dinten, L.C., Snijder, E.J., Gorbalenya, A.E., Ziebuhr, J., 2005. A complex zinc finger controls the enzymatic activities of nidovirus helicases. J. Virol. 79, 696–704.
Shah, N.R., Sunderland, A., Grdzelishvili, V.Z., 2010. Cell type mediated resistance of vesicular stomatitis virus and Sendai virus to ribavirin. PLoS One 5, e11265.
Shuman, S., Lima, C.D., 2004. The polynucleotide ligase and RNA capping enzyme superfamily of covalent nucleotidyltransferases. Curr. Opin. Struct. Biol. 14, 757–764.
Smith, E.C., Blanc, H., Surdel, M.C., Vignuzzi, M., Denison, M.R., 2013. Coronaviruses lacking exoribonuclease activity are susceptible to lethal mutagenesis: evidence for proofreading and potential therapeutics. PLoS Pathog. 9, e1003565.
Smith, E.C., Sexton, N.R., Denison, M.R., 2014. Thinking outside the triangle: replication fidelity of the largest RNA viruses. Annu. Rev. Virol. 1, 111–132.
Snijder, E.J., Kikkert, M., 2013. Arteriviruses. In: Knipe, D.M., Howley, P.M. (Eds.), Fields Virology. , 6th ed. Lippincott Williams & Wilkins, Philadelphia, PA, pp. 859–879.
Snijder, E.J., den Boon, J.A., Bredenbeek, P.J., Horzinek, M.C., Rijnbrand, R., Spaan, W.J., 1990. The carboxyl-terminal part of the putative Berne virus polymerase is expressed by ribosomal frameshifting and contains sequence motifs which indicate that toro- and coronaviruses are evolutionarily related. Nucleic Acids Res. 18, 4535–4542.
Snijder, E.J., Bredenbeek, P.J., Dobbe, J.C., Thiel, V., Ziebuhr, J., Poon, L.L., Guan, Y., Rozanov, M., Spaan, W.J., Gorbalenya, A.E., 2003. Unique and conserved features of genome and proteome of SARS-coronavirus, an early split-off from the coronavirus group 2 lineage. J. Mol. Biol. 331, 991–1004.
Snijder, E.J., Kikkert, M., Fang, Y., 2013. Arterivirus molecular biology and pathogenesis. J. Gen. Virol. 94, 2141–2163.
Snijder, E.J., Decroly, E., Ziebuhr, J., 2016. The nonstructural proteins directing Coronavirus RNA synthesis and processing. Adv. Virus Res. 96, 59–126.
Sola, I., Mateos-Gomez, P.A., Almazan, F., Zuniga, S., Enjuanes, L., 2011. RNA–RNA and RNA-protein interactions in coronavirus replication and transcription. RNA Biol. 8, 237–248.
Sola, I., Almazan, F., Zuniga, S., Enjuanes, L., 2015. Continuous and discontinuous RNA synthesis in Coronaviruses. Annu. Rev. Virol. 2, 265–288.
Spagnolo, J.F., Hogue, B.G., 2000. Host protein interactions with the 3' end of bovine coronavirus RNA and the requirement of the poly(A) tail for coronavirus defective genome replication. J. Virol. 74, 5053–5065.
Stroher, U., DiCaro, A., Li, Y., Strong, J.E., Aoki, F., Plummer, F., Jones, S.M., Feldmann, H., 2004. Severe acute respiratory syndrome-related coronavirus is inhibited by interferon- alpha. J. Infect. Dis. 189, 1164–1167.
Subissi, L., Imbert, I., Ferron, F., Collet, A., Coutard, B., Decroly, E., Canard, B., 2014a. SARS-CoV ORF1b-encoded nonstructural proteins 12–16: replicative enzymes as antiviral targets. Antiviral Res. 101, 122–130.
Subissi, L., Posthuma, C.C., Collet, A., Zevenhoven-Dobbe, J.C., Gorbalenya, A.E., Decroly, E., Snijder, E.J., Canard, B., Imbert, I., 2014b. One severe acute respiratory syndrome coronavirus protein complex integrates processive RNA polymerase and exonuclease activities. Proc. Natl. Acad. Sci. U. S. A. 111, E3900–3909.
Sutton, G., Fry, E., Carter, L., Sainsbury, S., Walter, T., Nettleship, J., Berrow, N., Owens, R., Gilbert, R., Davidson, A., Siddell, S., Poon, L.L., Diprose, J., Alderton, D., Walsh, M., Grimes, J.M., Stuart, D.I., 2004. The nsp9 replicase protein of SARS-coronavirus, structure and functional insights. Structure 12, 341–353.
Tan, E.L.C., Ooi, E.E., Lin, C.Y., Tan, H.C., Ling, A.E., Lim, B., Stanton, L.W., 2004. Inhibition of SARS coronavirus infection in vitro with clinically approved antiviral drugs. Emerg. Infect. Dis. 10, 581–586.
Tan, Y.W., Hong, W., Liu, D.X., 2012. Binding of the 5'-untranslated region of coronavirus RNA to zinc finger CCHC-type and RNA-binding motif 1 enhances viral replication and transcription. Nucleic Acids Res. 40, 5065–5077.
Tao, Y., Farsetta, D.L., Nibert, M.L., Harrison, S.C., 2002. RNA synthesis in a cage–structural studies of reovirus polymerase lambda3. Cell 111, 733–745.
te Velthuis, A.J., Fodor, E., 2016. Influenza virus RNA polymerase: insights into the mechanisms of viral RNA synthesis. Nat. Rev. Microbiol. 14, 479–493.
te Velthuis, A.J., Arnold, J.J., Cameron, C.E., van den Worm, S.H., Snijder, E.J., 2010a. The RNA polymerase activity of SARS-coronavirus nsp12 is primer dependent. Nucleic Acids Res. 38, 203–214.
te Velthuis, A.J., van den Worm, S.H., Sims, A.C., Baric, R.S., Snijder, E.J., van Hemert, M.J., 2010b. Zn(2 +) inhibits coronavirus and arterivirus RNA polymerase activity in vitro and zinc ionophores block the replication of these viruses in cell culture. PLoS Pathog. 6, e1001176.
te Velthuis, A.J., van den Worm, S.H., Snijder, E.J., 2012. The SARS-coronavirus nsp7 + nsp8 complex is a unique multimeric RNA polymerase capable of both de novo initiation and primer extension. Nucleic Acids Res. 40, 1737–1747.
te Velthuis, A.J., 2014. Common and unique features of viral RNA-dependent polymerases. Cell. Mol. Life Sci. 71, 4403–4420.
Thompson, A.A., Peersen, O.B., 2004. Structural basis for proteolysis-dependent activation of the poliovirus RNA-dependent RNA polymerase. EMBO J. 23, 3462–3471.
Tijms, M.A., van Dinten, L.C., Gorbalenya, A.E., Snijder, E.J., 2001. A zinc finger-containing papain-like protease couples subgenomic mRNA synthesis to genome translation in a positive-stranded RNA virus. Proc. Natl. Acad. Sci. U. S. A. 98, 1889–1894.
van Dinten, L.C., den Boon, J.A., Wassenaar, A.L., Spaan, W.J., Snijder, E.J., 1997. An infectious arterivirus cDNA clone: identification of a replicase point mutation that abolishes discontinuous mRNA transcription. Proc. Natl. Acad. Sci. U. S. A. 94, 991–996.
van Hemert, M.J., de Wilde, A.H., Gorbalenya, A.E., Snijder, E.J., 2008a. The in vitro RNA synthesizing activity of the isolated arterivirus replication/transcription complex is dependent on a host factor. J. Biol. Chem. 283, 16525–16536.
van Hemert, M.J., van den Worm, S.H., Knoops, K., Mommaas, A.M., Gorbalenya, A.E., Snijder, E.J., 2008b. SARS-coronavirus replication/transcription complexes are membrane-protected and need a host factor for activity in vitro. PLoS Pathog. 4, e1000054.
van Vliet, A.L., Smits, S.L., Rottier, P.J., de Groot, R.J., 2002. Discontinuous and non-discontinuous subgenomic RNA transcription in a nidovirus. EMBO J. 21, 6571–6580.
van der Hoeven, B., Oudshoorn, D., Koster, A.J., Snijder, E.J., Kikkert, M., Barcena, M., 2016. Biogenesis and architecture of arterivirus replication organelles. Virus Res. 220, 70–90.
von Brunn, A., Teepe, C., Simpson, J.C., Pepperkok, R., Friedel, C.C., Zimmer, R., Roberts, R., Baric, R., Haas, J., 2007. Analysis of intraviral protein–protein interactions of the SARS coronavirus ORFeome. PLoS One 2, e459.
Warren, T.K., Wells, J., Panchal, R.G., Stuthman, K.S., Garza, N.L., Van Tongeren, S.A., Dong, L., Retterer, C.J., Eaton, B.P., Pegoraro, G., Honnold, S., Bantia, S., Kotian, P., Chen, X., Taubenheim, B.R., Welch, L.S., Minning, D.M., Babu, Y.S., Sheridan,

W.P., Bavari, S., 2014. Protection against filovirus diseases by a novel broad-spectrum nucleoside analogue BCX4430. Nature 508, 402–405.
Warren, T.K., Jordan, R., Lo, M.K., Ray, A.S., Mackman, R.L., Soloveva, V., Siegel, D., Perron, M., Bannister, R., Hui, H.C., Larson, N., Strickley, R., Wells, J., Stuthman, K.S., Van Tongeren, S.A., Garza, N.L., Donnelly, G., Shurtleff, A.C., Retterer, C.J., Gharaibeh, D., Zamani, R., Kenny, T., Eaton, B.P., Grimes, E., Welch, L.S., Gomba, L., Wilhelmsen, C.L., Nichols, D.K., Nuss, J.E., Nagle, E.R., Kugelman, J.R., Palacios, G., Doerffler, E., Neville, S., Carra, E., Clarke, M.O., Zhang, L., Lew, W., Ross, B., Wang, Q., Chun, K., Wolfe, L., Babusis, D., Park, Y., Stray, K.M., Trancheva, I., Feng, J.Y., Barauskas, O., Xu, Y., Wong, P., Braun, M.R., Flint, M., McMullan, L.K., Chen, S.S., Fearns, R., Swaminathan, S., Mayers, D.L., Spiropoulou, C.F., Lee, W.A., Nichol, S.T., Cihlar, T., Bavari, S., 2016. Therapeutic efficacy of the small molecule GS-5734 against Ebola virus in rhesus monkeys. Nature 531, 381–385.
Weiss, S.R., Leibowitz, J.L., 2011. Coronavirus pathogenesis. Adv. Virus Res. 81, 85–164.
Weiss, R.C., Oostrom-Ram, T., 1989. Inhibitory effects of ribavirin alone or combined with human alpha interferon on feline infectious peritonitis virus replication in vitro. Vet. Microbiol. 20, 255–265.
Weng, L., Weersink, A., Poljak, Z., de Lange, K., von Massow, M., 2016. An economic evaluation of intervention strategies for Porcine Epidemic Diarrhea (PED). Prev. Vet. Med. 134, 58–68.
Wu, C.H., Chen, P.J., Yeh, S.H., 2014. Nucleocapsid phosphorylation and RNA helicase DDX1 recruitment enables coronavirus transition from discontinuous to continuous transcription. Cell Host Microbe 16, 462–472.
Xiao, Y., Ma, Q., Restle, T., Shang, W., Svergun, D.I., Ponnusamy, R., Sczakiel, G., Hilgenfeld, R., 2012. Nonstructural proteins 7 and 8 of feline coronavirus form a 2:1 heterotrimer that exhibits primer-independent RNA polymerase activity. J. Virol. 86, 4444–4454.
Xu, X., Liu, Y., Weiss, S., Arnold, E., Sarafianos, S.G., Ding, J., 2003. Molecular model of SARS coronavirus polymerase: implications for biochemical functions and drug design. Nucleic Acids Res. 31, 7117–7130.
Yang, D., Leibowitz, J.L., 2015. The structure and functions of coronavirus genomic 3' and 5' ends. Virus Res. 206, 120–133.
Yang, J., Yan, R., Roy, A., Xu, D., Poisson, J., Zhang, Y., 2015. The I-TASSER Suite: protein structure and function prediction. Nat. Methods 12, 7–8.
Yount, B., Roberts, R.S., Lindesmith, L., Baric, R.S., 2006. Rewiring the severe acute respiratory syndrome coronavirus (SARS-CoV) transcription circuit: engineering a recombination-resistant genome. Proc. Natl. Acad. Sci. U. S. A. 103, 12546–12551.
Züst, R., Miller, T.B., Goebel, S.J., Thiel, V., Masters, P.S., 2008. Genetic interactions between an essential 3' cis-acting RNA pseudoknot, replicase gene products, and the extreme 3' end of the mouse coronavirus genome. J. Virol. 82, 1214–1228.
Zeng, Q.L., Zhang, J.Y., Zhang, Z., Wang, L.F., Wang, F.S., 2013. Sofosbuvir and ABT-450: terminator of hepatitis C virus? World J. Gastroenterol. 19, 3199–3206.
Zhai, Y., Sun, F., Li, X., Pang, H., Xu, X., Bartlam, M., Rao, Z., 2005. Insights into SARS-CoV transcription and replication from the structure of the nsp7-nsp8 hexadecamer. Nat. Struct. Mol. Biol. 12, 980–986.
Zhang, J., 2016. Porcine deltacoronavirus Overview of infection dynamics, diagnostic methods, prevalence and genetic evolution. Virus Res. 226, 71–84.
Zheng, H., Zhang, K., Zhu, X.Q., Liu, C., Lu, J., Gao, F., Zhou, Y., Zheng, H., Lin, T., Li, L., Tong, G., Wei, Z., Yuan, S., 2014. Genetic manipulation of a transcription-regulating sequence of porcine reproductive and respiratory syndrome virus reveals key nucleotides determining its activity. Arch. Virol. 159, 1927–1940.
Ziebuhr, J., Snijder, E.J., Gorbalenya, A.E., 2000. Virus-encoded proteinases and proteolytic processing in the Nidovirales. J. Gen. Virol. 81, 853–879.
Zuniga, S., Sola, I., Alonso, S., Enjuanes, L., 2004. Sequence motifs involved in the regulation of discontinuous coronavirus subgenomic RNA synthesis. J. Virol. 78, 980–994.
Zuo, Y., Deutscher, M.P., 2001. Exoribonuclease superfamilies: structural analysis and phylogenetic distribution. Nucleic Acids Res. 29, 1017–1026.